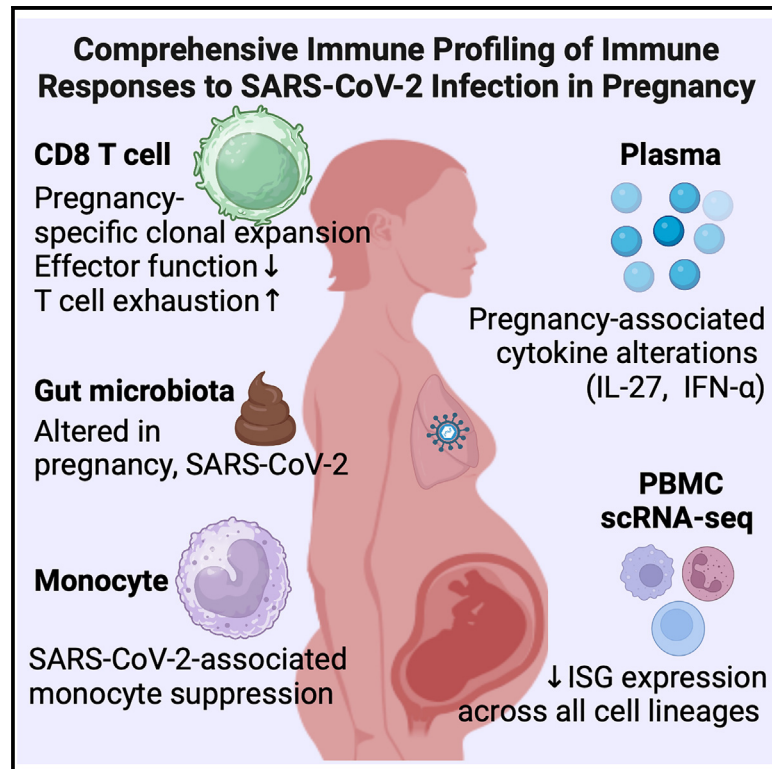


SARS-CoV-2 infection elucidates features of pregnancy-specific immunity

Graphical abstract



Authors

Dong Sun Oh, Eunha Kim, Rachelly Normand, ..., Alexandra-Chloé Villani, Andrea G. Edlow, Jun R. Huh

Correspondence

avillani@mgh.harvard.edu (A.-C.V.), aedlow@mgh.harvard.edu (A.G.E.), jun_huh@hms.harvard.edu (J.R.H.)

In brief

Oh et al. perform a comprehensive immune survey of COVID-19 in pregnant and non-pregnant women, identifying pregnancy-specific alterations in immune responses. These include altered T cell responses, monocyte function, chemokines and cytokines, and gut microbial composition. This work provides insights into how pregnancy shapes antiviral immunity.

Highlights

- COVID-19 is associated with altered T cell responses in pregnant patients
- Identified altered cytokine and chemokine levels in pregnant patients with COVID-19
- scRNA-seq analyses reveal decreased ISG responses in pregnant patients with COVID-19
- Severe/critical illness and maternal obesity are associated with additional immune dysfunction



Resource

SARS-CoV-2 infection elucidates features of pregnancy-specific immunity

Dong Sun Oh,^{1,31} Eunha Kim,^{1,2,31} Rachelly Normand,^{3,4,5,6,31} Guangqing Lu,^{1,31} Lydia L. Shook,^{7,8} Amanda Lyall,^{9,10} Olyvia Jasset,⁸ Stepan Demidkin,⁸ Emily Gilbert,⁸ Joon Kim,⁸ Babatunde Akinwunmi,⁸ Jessica Tantivit,^{3,4,5} Alice Tirard,^{3,4,5} Benjamin Y. Arnold,^{3,4,5} Kamil Slowikowski,^{3,4,5,6} MGH COVID-19 Collection & Processing Team, Marcia B. Goldberg,^{5,11,12,13} Michael R. Filbin,^{5,14} Nir Hacohen,^{4,5,15} Long H. Nguyen,^{16,17,18}

(Author list continued on next page)

¹Department of Immunology, Blavatnik Institute, Harvard Medical School, Boston, MA 02115, USA

²BK21 Graduate Program, Department of Biomedical Sciences and Department of Neuroscience, Korea University College of Medicine, Seoul 02841, Republic of Korea

³Center for Immunology and Inflammatory Diseases, Department of Medicine, Massachusetts General Hospital, Boston, MA 02129, USA

⁴Krantz Family Center for Cancer Research, Massachusetts General Hospital, Boston, MA 02114, USA

⁵Broad Institute of MIT and Harvard, Cambridge, MA 02142, USA

⁶Harvard Medical School, Boston, MA 02115, USA

⁷Department of Obstetrics, Gynecology and Reproductive Biology, Massachusetts General Hospital, Harvard Medical School, Boston, MA 02114, USA

⁸Vincent Center for Reproductive Biology, Massachusetts General Hospital, Boston, MA 02114, USA

⁹Department of Psychiatry, Brigham and Women's Hospital, Harvard Medical School, Boston, MA 02115, USA

¹⁰Department of Psychiatry, Massachusetts General Hospital, Harvard Medical School, Boston, MA 02114, USA

¹¹Division of Infectious Diseases, Department of Medicine, Massachusetts General Hospital, Boston, MA 02114, USA

¹²Department of Microbiology, Harvard Medical School, Boston, MA 02115, USA

¹³Harvard T.H. Chan School of Public Health, Boston, MA 02115, USA

¹⁴Department of Emergency Medicine, Massachusetts General Hospital, Harvard Medical School, Boston, MA 02114, USA

¹⁵Department of Medicine, Harvard Medical School, Boston, MA 02115, USA

¹⁶Division of Gastroenterology, Massachusetts General Hospital and Harvard Medical School, Boston, MA 02114, USA

¹⁷Clinical and Translational Epidemiology Unit, Massachusetts General Hospital and Harvard Medical School, Boston, MA 02114, USA

¹⁸Harvard Chan Microbiome in Public Health Center, Harvard T.H. Chan School of Public Health, Boston, MA 02115, USA

¹⁹Department of Immunology and Infectious Diseases, Harvard T.H. Chan School of Public Health, Boston, MA 02115, USA

²⁰Infectious Disease Division, Brigham and Women's Hospital, Boston, MA 02115, USA

²¹Ragon Institute of MGH, MIT and Harvard, Cambridge, MA 02139, USA

²²Division of Infectious Diseases, Brigham and Women's Hospital, Boston, MA 02115, USA

(Affiliations continued on next page)

SUMMARY

Pregnancy is a risk factor for increased severity of severe acute respiratory syndrome coronavirus 2 (SARS-CoV-2) and other respiratory infections, but the mechanisms underlying this risk are poorly understood. To gain insight into the role of pregnancy in modulating immune responses at baseline and upon SARS-CoV-2 infection, we collected peripheral blood mononuclear cells and plasma from 226 women, including 152 pregnant individuals and 74 non-pregnant women. We find that SARS-CoV-2 infection is associated with altered T cell responses in pregnant women, including a clonal expansion of CD4-expressing CD8⁺ T cells, diminished interferon responses, and profound suppression of monocyte function. We also identify shifts in cytokine and chemokine levels in the sera of pregnant individuals, including a robust increase of interleukin-27, known to drive T cell exhaustion. Our findings reveal nuanced pregnancy-associated immune responses, which may contribute to the increased susceptibility of pregnant individuals to viral respiratory infection.

INTRODUCTION

Coronavirus disease 2019 (COVID-19) is a respiratory infectious disease caused by severe acute respiratory syndrome coronavirus 2 (SARS-CoV-2).^{1–3} The COVID-19 global pandemic has resulted in hundreds of millions of infections, including over 200,000 pregnant women in the United States.⁴ In severe or critical COVID-19,

non-pregnant patients often exhibit aberrant activation of innate and adaptive immune responses,^{5,6} leading to a profound functional alteration of immune cells.^{7,8} For example, aggravated inflammatory responses accompanied by a massive increase in inflammatory cytokines are one of the key features of COVID-19, which is also closely correlated with disease severity.^{9–14} An increase in regulatory T cell (Treg) levels has been observed,^{15,16}



Andrew T. Chan,^{16,17,18,19} Xu G. Yu,^{20,21} Jonathan Z. Li,²² Lael Yonker,²³ Alessio Fasano,²⁴ Roy H. Perlis,^{16,17} Ofer Pasternak,^{9,10,25} Kathryn J. Gray,²⁶ Gloria B. Choi,²⁷ David A. Drew,^{16,17} Pritha Sen,^{3,5,6,28,29,30} Alexandra-Chloé Villani,^{3,4,5,6,30,*} Andrea G. Edlow,^{7,8,30,*} and Jun R. Huh^{1,30,32,*}

²³Mucosal Immunology and Biology Research Center, Massachusetts General Hospital, Boston, MA 02114, USA

²⁴Division of Pediatric Gastroenterology and Nutrition, Massachusetts General Hospital, Boston, MA 02114, USA

²⁵Department of Radiology, Brigham and Women's Hospital, Harvard Medical School, Boston, MA 02115, USA

²⁶Department of Obstetrics & Gynecology, University of Washington, Seattle, WA 98195, USA

²⁷The Picower Institute for Learning and Memory, Department of Brain and Cognitive Sciences, Massachusetts Institute of Technology, Cambridge, MA 02139, USA

²⁸Transplant, Oncology, and Immunocompromised Host Group, Division of Infectious Diseases, Brigham and Women's Hospital, Boston, MA 02115, USA

²⁹Dana-Farber Cancer Institute, Boston, MA 02215, USA

³⁰Senior author

³¹These authors contributed equally

³²Lead contact

*Correspondence: avillani@mgh.harvard.edu (A.-C.V.), aedlow@mgh.harvard.edu (A.G.E.), jun_huh@hms.harvard.edu (J.R.H.)
<https://doi.org/10.1016/j.celrep.2024.114933>

presumably as a compensatory mechanism to dampen immune responses. Additionally, an exhausted T cell phenotype with upregulated inhibitory receptor expression has been reported, particularly in those with severe or critical disease.¹⁷

While many studies have characterized immune responses to COVID-19 that are associated with disease progression in non-pregnant populations,^{5,18–21} substantially less is known about immune responses to COVID-19 in pregnancy,^{22–27} despite the clinical observation that pregnant individuals are at increased risk for severe COVID-19-associated morbidity and mortality.²⁸ Pregnant individuals with COVID-19 are significantly more likely than age-matched non-pregnant individuals to require an intensive care unit admission, invasive ventilation, and extracorporeal membrane oxygenation.^{29–31} COVID-19 has also been associated with pregnancy-specific complications, including higher rates of preterm birth, postpartum hemorrhage, hypertensive disorders of pregnancy, and thrombotic events, resulting in increased maternal morbidity and mortality, as well as neonatal complications.^{32–34} Furthermore, earlier studies suggested that hyperactivation of the maternal immune system might put fetuses at risk for adverse neurodevelopmental or metabolic programming.^{35–37} Therefore, understanding the characteristics of pregnancy-specific viral immune responses is critical to developing effective treatments for pregnant individuals and to reducing pregnancy-associated severe morbidity, mortality, and other complications for SARS-CoV-2 specifically and, more broadly, for other viruses that may impact pregnant individuals and their offspring.

Pregnancy poses unique challenges to the maternal immune system, which is tasked with tolerating the fetus while simultaneously protecting pregnant individuals and the developing fetus from invading pathogens.^{37–39} Altered cytokine expression has been reported in pregnant individuals with COVID-19, relative to uninfected pregnant women.^{32–34,40} Studies of pregnancy-associated immune changes in COVID-19, however, have reported varied results.⁴¹ For example, while some studies reported altered T cell activation in SARS-CoV-2-infected pregnant women compared to non-pregnant individuals,^{42,43} others indicated comparable responses.^{23,44} In addition, studies have reported conflicting results regarding augmented versus downregulated function of circulating monocytes in pregnant women with SARS-CoV-2 infection.^{43,45,46} These disparate findings might be attributed to

heterogeneity and imprecise phenotyping of pregnant women's clinical presentations across studies. Some of these studies lacked sufficient sample size and patient diversity to account for key clinical factors such as disease severity, interval since infection, and comorbidities such as obesity, which influence immune responses. Furthermore, prior research often focused narrowly on specific immune features rather than comprehensive profiling of diverse immune cell populations and their responses. Finally, few studies have comprehensively profiled the pregnancy-specific SARS-CoV-2 response, including critical comparator groups such as pregnant uninfected controls, non-pregnant controls, and non-pregnant individuals with COVID-19.

To address these critical gaps, we comprehensively assessed the differences between host immune responses to SARS-CoV-2 in pregnant women and non-pregnant women, including the effects of disease severity, phase of illness, and obesity, the most common pregnancy comorbidity impacting the maternal host immune response. We also considered fetal sex in our analyses, which has been demonstrated to influence maternal and placental immune responses to SARS-CoV-2.²⁴ We collected peripheral blood mononuclear cells (PBMCs), plasma, and stool from unvaccinated pregnant individuals with or without first-time SARS-CoV-2 infection, and non-pregnant women with or without first-time SARS-CoV-2 infection (Tables S1, S2, and S3) as controls. Using flow cytometry, single-cell multiomics, *ex vivo* immune cell stimulation, and unbiased immune correlative analyses, we performed comparative analyses aimed at defining pregnancy-associated immune changes during and following SARS-CoV-2 infection. Our findings highlight mechanisms by which pregnancy influences maternal host immune responses against viral infection. Our work provides a mechanistic framework that enables a comprehensive understanding of the impact of SARS-CoV-2 infection in pregnancy on the short- and longer-term immunity of both mothers and offspring.

RESULTS

Comparative immune cell analyses of non-pregnant versus pregnant women with COVID-19

To decipher the critical immunological drivers shaping the host immune responses in pregnant women infected with

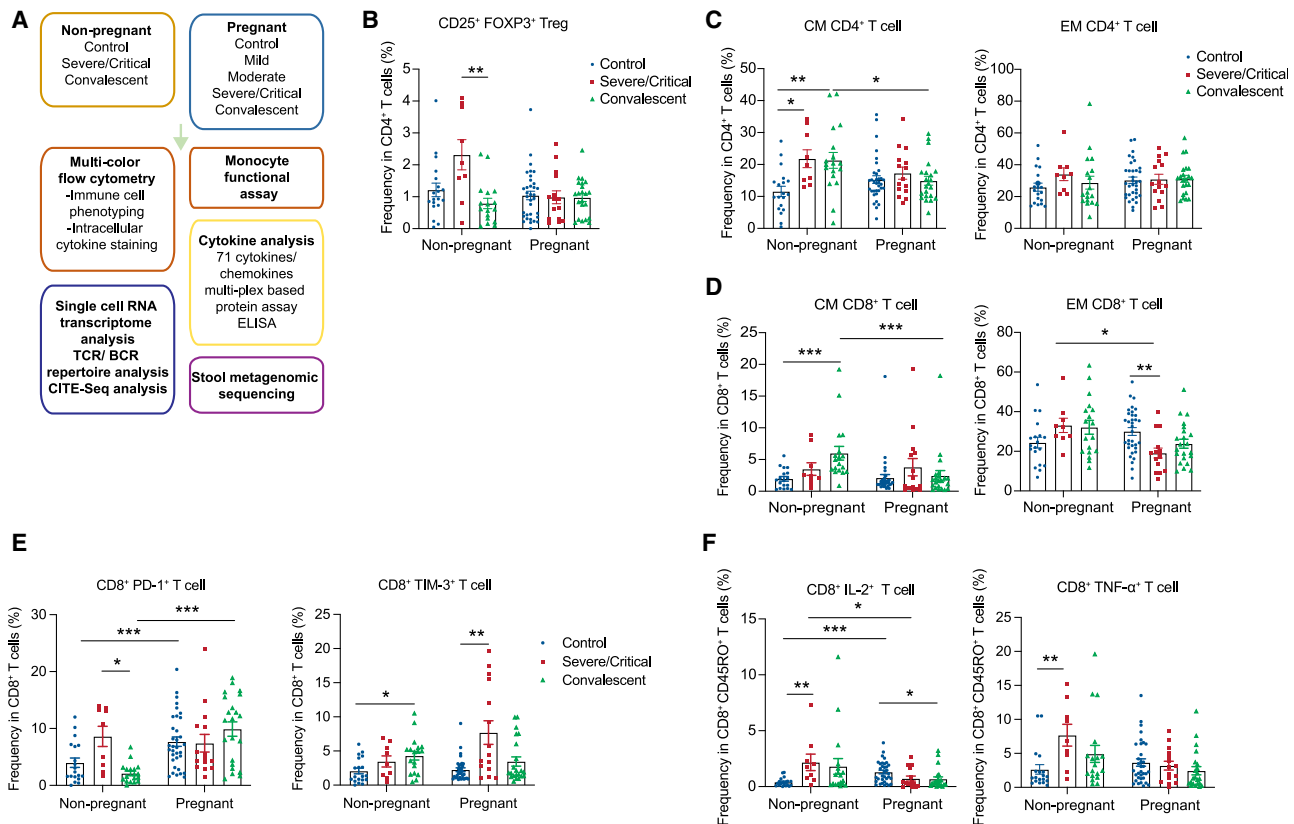


Figure 1. Comparative T cell analyses of pregnant versus non-pregnant patients with COVID-19

(A) A schematic of the analyses performed in this paper: non-pregnant versus pregnant women with or without COVID-19.

(B) CD25⁺ FOXP3⁺-expressing CD4⁺ T cell frequencies in PBMCs.

(C and D) Left panels show CM (CD45RO⁺ CCR7⁺) and right panels show EM (CD45RO⁺ CCR7⁻) frequencies in CD4⁺ T cells (CD19⁻ CD3⁺ CD4⁺) (C) and CD8⁺ (CD19⁻ CD3⁺ CD8⁺) T cells (D) in PBMCs.

(E and F) Frequencies of CD8⁺ T cells expressing (E) PD-1 and Tim-3 and (F) IL-2 and TNF- α . Healthy (non-pregnant, $n = 19$; pregnant, $n = 34$), severe/critical COVID-19 (non-pregnant, $n = 9$; pregnant, $n = 15$), or convalescent COVID-19 (non-pregnant, $n = 18$; pregnant, $n = 22$). Data are shown as the mean \pm SEM. * $p < 0.05$, ** $p < 0.01$, *** $p < 0.001$.

SARS-CoV-2, PBMCs, plasma, and stool samples were collected from 226 women, including 152 pregnant and 74 non-pregnant women (Tables S1, S2, and S3). During the height of the COVID-19 pandemic (April 2020 to January 2021), samples were prospectively collected from pregnant, unvaccinated women (see STAR Methods) who had mild, moderate, and severe/critical COVID-19 (severity determinations were categorized as per NIH criteria^{47,48}) and from uninfected contemporaneously pregnant controls (SARS-CoV-2 PCR negative). Samples were collected during the period of acute illness (within 30 days of positive SARS-CoV-2 PCR test) and/or during the convalescent period (>30 days after positive PCR test; see STAR Methods). PBMCs from non-pregnant women with COVID-19 and from uninfected non-pregnant controls of similar age groups were analyzed as additional comparator groups. We performed flow cytometry analyses to profile immune cell composition and intracellular cytokine expression across 156 PBMC specimens (Figure 1A; Figures S1A and S1B; Tables S1, S2, and S3).

Uncontrolled inflammatory responses are closely associated with poorer outcomes in COVID-19.^{49–54} Tregs are often respon-

sible for restraining excessive immune responses, and previous work has found that Treg frequencies were increased in severe COVID-19 patients.⁵⁵ Tregs also play critical roles in maintaining maternal-fetal tolerance,^{56–58} and impairment of such tolerance leads to adverse pregnancy outcomes.^{59–61} Thus, we analyzed FOXP3⁺ CD25⁺ Treg frequencies among CD4⁺ T cells in PBMCs across six different groups consisting of non-pregnant and pregnant patients across three subgroups (control, severe, and convalescent). Consistent with a previous report,⁵⁵ our data indicated Treg frequencies were increased in severe/critical non-pregnant COVID-19 cases and were reduced to baseline, uninfected levels in the convalescent phase (Figure 1B). In contrast to these findings in non-pregnant women, in pregnant women, Treg frequencies did not increase with severe/critical COVID-19 (Figure 1B), suggesting altered Treg responses following viral infection.

We next analyzed other immune cell frequencies among total live cells. Major populations such as T cell, B cell, monocyte, natural killer (NK), and natural killer T (NKT) cell levels among total live cells were comparable between non-pregnant

and pregnant women regardless of their infection status or severity (Figure S2A). To investigate pregnancy-associated changes within a specific cell type, we analyzed cell frequencies at the subpopulation level. Consistent with the percentage comparison among total live cells, we found T cell, B cell, and basophil frequencies were comparable between non-pregnant and pregnant women with COVID-19 regardless of their disease severity (Figure S2B). While granulocytes are usually excluded from the PBMC preparation, earlier reports indicated that low-density neutrophil and eosinophil levels correlate with the severity of COVID-19 in non-pregnant individuals.^{62–64} We also found that neutrophil frequency within the CD3⁺CD56⁺CD66b⁺ population was significantly decreased in convalescent pregnant patients relative to convalescent non-pregnant individuals (Figure S2B). We found a significant increase in NK cell frequencies in severe/critical COVID-19 in pregnancy, compared to pregnant controls. In contrast, there were no COVID-19-associated changes in NK cell frequencies in the non-pregnant group (Figure S2B). While NKT cell levels were increased in non-pregnant participants during COVID-19 convalescence, their levels were significantly decreased in the pregnant convalescent group compared to the severe/critical disease group. An increase in the $\gamma\delta$ T cell percentage was previously reported in pregnant control women,⁶⁵ and a decrease in $\gamma\delta$ T cell frequency has been noted in patients with COVID-19.⁶⁶ Consistent with prior findings, we observed that pregnant controls had significantly increased $\gamma\delta$ T cell frequencies compared to uninfected non-pregnant women, and SARS-CoV-2 infection was associated with reduced $\gamma\delta$ T cell fractions in both groups (Figure S2C). Unlike the non-pregnant groups, however, $\gamma\delta$ T cell levels were not restored to the basal level in pregnant convalescent women (Figure S2C). These data indicate that the composition of various immune cell types is largely comparable between pregnant and non-pregnant groups.

Pregnancy-dependent changes in T cell function

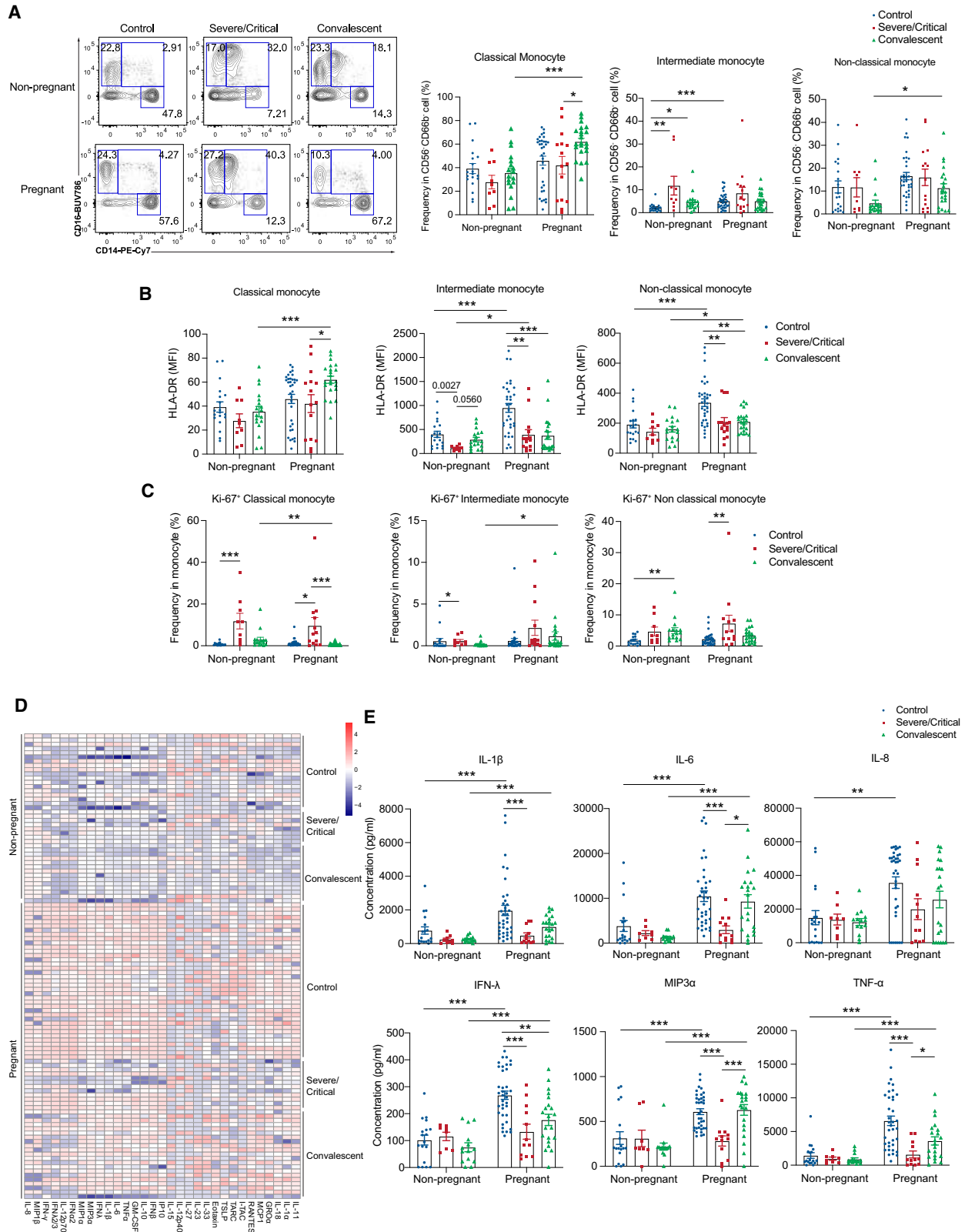
We next investigated whether pregnancy was associated with altered T cell activation and function in the setting of COVID-19. First, we analyzed major T cell subpopulations defined by CCR7 and CD45RO expression level measured by flow cytometry. In non-pregnant women with COVID-19, the percentage of the central memory (CM, CD45RO⁺, CCR7⁺) subset of CD4⁺ T cells was significantly increased in the severe/critical and convalescent COVID-19 subjects compared with uninfected non-pregnant controls (Figure 1C). CM CD8⁺ T cell levels were significantly increased in non-pregnant convalescent women compared with uninfected controls (Figure 1D). Such changes were not observed in the pregnant group. Pregnant convalescent individuals had significantly lower frequencies of CM CD4⁺ and CD8⁺ T cells relative to non-pregnant convalescent women (Figures 1C and 1D). Effector memory (EM, CD45RO⁺, CCR7⁻) CD8⁺ T cell percentages were lower in the pregnant patients with COVID-19 relative to both pregnant uninfected controls and non-pregnant women with COVID-19 (Figure 1D). These data indicate that the EM CD8⁺ T cell response, one of the most important T cell subsets for antiviral immune responses,^{67,68} was likely impaired in pregnant women with COVID-19. Furthermore, reduced percentages of the CM CD8⁺

T cells in the pregnant convalescent group may indicate that the maintenance of CM CD8⁺ T cell function was impaired in pregnant women following COVID-19.

T cell exhaustion and associated functional impairment phenotypes have previously been reported in patients with COVID-19⁶ characterized by the upregulation of inhibitory receptors, such as programmed cell death protein 1 (PD-1) and Tim-3.^{69,70} In addition, upregulation of PD-1 and Tim-3 in peripheral leukocytes has also been noted in normal pregnancy and is thought to be associated with maternal-fetal immune tolerance.⁷⁰ Consistent with these prior findings, PD-1 expression was increased in CD8⁺ T cells in the pregnant uninfected control and pregnant convalescent groups, compared with their non-pregnant control and convalescent counterparts (Figure 1E). SARS-CoV-2 infection was associated with increased T cell exhaustion in pregnant patients with severe/critical COVID-19, as indicated by significantly increased TIM-3 levels compared to pregnant uninfected controls (Figure 1E). These data indicate that CD8⁺ T cell function may be impaired in the pregnant group.

We further assessed the impact of pregnancy on T cell function by measuring the production of cytokines upon *in vitro* stimulation of PBMCs with phorbol 12-myristate 13-acetate (PMA) and ionomycin. We found that, unlike non-pregnant patients with COVID-19, interleukin (IL)-2 and tumor necrosis factor- α (TNF- α) production by CD45RO⁺CD8⁺ T cells in pregnant patients with COVID-19 were not increased compared to control groups (Figure 1F). Severe/critical COVID-19 induced increased production of IL-2, TNF- α , interferon (IFN)- γ , and granzyme B by CD45RO⁺CD4⁺ T cells in the non-pregnant group (Figure S3A). Such an increase was not observed in pregnant women with COVID-19. Production of IL-17A, however, was significantly increased in the setting of severe/critical COVID-19 in pregnant women only (Figure S3A). We also noted that $\gamma\delta$ T cells from pregnant women with COVID-19 produced increased levels of IFN- γ compared to control pregnant women (Figure S3B). These data suggest that CD8⁺ T cell function may be impaired in pregnant women due to the enhanced expression of co-inhibitory molecules, which may serve as a contributing factor to predispose pregnant women to increased disease severity in the setting of COVID-19. Conversely, T helper (Th)17 cell function seems to be enhanced in the setting of viral infection in pregnancy, echoing earlier findings from inflammation-exposed pregnant rodent work.^{71–73}

To better understand COVID-19 severity within the pregnant individuals (Tables S1, S2, and S3), we next compared T cell function within pregnant groups depending on COVID-19 severity. Compared to other groups, EM CD4⁺ and EM CD8⁺ T cell frequencies were altered in the moderate and severe/critical groups, respectively (Figures S4A and S4B). Upon *in vitro* stimulation, CD4⁺ T cells isolated from the moderate group produced the highest amounts of IFN- γ , TNF- α , and granzyme B, compared to other groups, including the severe/critical group (Figure S4C). Such moderate group-associated robust cytokine production was not observed in IL-17A-producing CD4⁺ cells (Figure S4D). IFN- γ -producing CD8⁺ T cell level was also highest in the moderate group (Figure S4E). On the other hand, IFN- γ - and TNF- α -producing $\gamma\delta$ T cell levels were strongly induced in the mild, not moderate, COVID-19 group (Figure S4F).



(legend on next page)

Taken together, these data indicate that SARS-CoV-2 infection and pregnancy led to altered immune cell function, which was more pronounced in CD4⁺ and CD8⁺ T cells depending on disease severity.

Pregnancy-dependent changes in monocyte function

We next assessed whether pregnancy and COVID-19 were associated with alterations in monocyte composition and function. Three major populations of monocytes can be defined by flow cytometry in blood based on the level of CD14 and CD16 expression: classical monocytes, CD14⁺CD16⁻; intermediate monocytes, CD14⁺CD16⁺; and non-classical monocytes, CD14^{low}CD16⁺.^{74,75} Classical monocyte levels were highest in pregnant convalescent women compared to other groups (Figure 2A). Levels of intermediate monocytes were increased in non-pregnant individuals with severe/critical COVID-19 relative to uninfected controls (Figure 2A); this increase was not observed in pregnant individuals. Finally, non-classical monocyte frequencies were significantly higher in pregnant convalescent women compared to non-pregnant convalescent women (Figure 2A).

We further examined monocyte expression of human leukocyte antigen-DR (HLA-DR), a major histocompatibility complex (MHC) class II surface receptor that presents antigens to T cells. Earlier studies of patients with severe COVID-19 identified reduced HLA-DR expression on monocytes as a marker for immune suppression and monocyte exhaustion.^{7,8,76–78} In intermediate and non-classical monocytes, HLA-DR expression levels were higher at baseline in the pregnant uninfected controls compared to non-pregnant controls. HLA-DR expression was significantly reduced in the setting of severe/critical COVID-19 relative to uninfected controls in both pregnant and non-pregnant groups (Figure 2B). Intriguingly, in pregnant individuals, HLA-DR expression was restored during convalescence in classical monocytes only, while it remained suppressed even in convalescence in intermediate and non-classical monocytes. Moreover, HLA-DR expression in both classical and non-classical monocytes was significantly higher in the pregnant convalescent group relative to non-pregnant convalescent individuals (Figure 2B). Taken together, these findings suggest that pregnant individuals may have heightened antigen-presenting monocyte capabilities compared to non-pregnant individuals, with antigen-presenting capacity of monocytes significantly reduced in the setting of severe or critical COVID-19. The observed reduction in HLA-DR expression likely reflected monocyte exhaustion rather than reduced monocyte proliferation, as staining with the active proliferation marker Ki67 revealed robust proliferation of classical and non-classical monocytes during the acute phase of COVID-19 in both non-pregnant and pregnant patients (Figure 2C). In aggregate, these data indicate that

pregnancy itself alters the relative abundance of certain circulating monocyte subsets, and thus the monocyte exhaustion associated with severe/critical COVID-19 may have a differential impact on the antigen-presenting capabilities of pregnant individuals and therefore their ability to activate specific T cell responses.

To test monocyte function in pregnant individuals with and without COVID-19, we enriched monocytes from PBMCs, followed by *ex vivo* activation with a low amount of an immune stimulant, lipopolysaccharide (LPS). For this stimulation assay, we selected the concentration of LPS that did not trigger robust cytokine responses in CD14⁺ monocytes isolated from the non-pregnant uninfected controls (Figure 2D). Intriguingly, CD14⁺ monocytes from pregnant uninfected individuals produced higher mean levels of many cytokines compared to CD14⁺ monocytes from all non-pregnant groups (Figure 2D). In the setting of COVID-19, however, particularly in severe/critical patients, cytokine production by monocytes from pregnant individuals was significantly dampened relative to the pregnant uninfected baseline and relative to convalescent pregnant individuals (Figure 2E). For example, IL-1 β , IL-6, IFN- λ , CC chemokine ligand 20 (CCL20, MIP3a), and TNF- α levels were significantly reduced in pregnant patients with severe/critical COVID-19 relative to uninfected pregnant controls and were comparable between the pregnant severe/critical COVID-19 patients and the non-pregnant groups (Figure 2E). In sharp contrast to non-pregnant individuals, pregnant convalescent patients' monocytes regained the ability to produce high amounts of many cytokines (e.g., IL-1 β , IL-6, MIP3a, and TNF- α) (Figure 2E). We then compared monocyte function among pregnant women with different disease severity. While monocytes from the convalescent group display enhanced MIP3a and IL-6 production compared to the severe/critical group (Figure S5A), SARS-CoV-2 infection in pregnancy led to a prolonged suppressive effect on monocyte function, as shown by significantly reduced production of IL-12p70, IFN- α , and IFN- γ (Figure S5B). Thus, monocytes from pregnant individuals demonstrated an enhanced ability to produce cytokines at baseline, which was robustly suppressed by severe/critical COVID-19 to a greater extent than monocytes from non-pregnant counterparts. Of note, monocytes from pregnant individuals recovered their cytokine-producing function in convalescence, while such recovery was not observed in monocytes from non-pregnant individuals.

Immune responses associated with pregnancy defined by single-cell RNA sequencing of PBMCs from pregnant women with COVID-19

To gain an unbiased understanding of the differences in host immune responses between pregnant and non-pregnant patients

Figure 2. Pregnancy enhances monocyte function

(A) Representative fluorescence-activated cell sorting (FACS) plots and quantifications of classical monocytes (CD14⁺), intermediate monocytes (CD14⁺CD16⁺), and non-classical monocytes (CD16⁺) as analyzed by flow cytometry from PBMCs.
(B) Mean fluorescence intensities (MFIs) of HLA-DR expression in classical, intermediate, and alternative monocytes.
(C) Frequencies of Ki67, a proliferation marker, expressed in classical, intermediate, and alternative monocytes.
(D and E) A heatmap presenting monocyte-secreted cytokines upon 1 ng/mL LPS stimulation (D) and representative cytokine levels in the supernatant as quantified by cytometric bead array analyses (E). Healthy (non-pregnant, $n = 19$; pregnant, $n = 34$), severe/critical COVID-19 (non-pregnant, $n = 9$; pregnant, $n = 15$), or convalescent COVID-19 (non-pregnant, $n = 18$; pregnant, $n = 22$). Data are shown as the mean \pm SEM. * $p < 0.05$, ** $p < 0.01$, *** $p < 0.001$.

with COVID-19, we performed single-cell RNA sequencing (scRNA-seq) with cellular indexing of transcriptomes and epitope sequencing (CITE-seq) on 26 PBMC samples, including those from pregnant patients with severe COVID-19, asymptomatic COVID-19, or no SARS-CoV-2 infection, as well as age- and sex-matched controls from non-pregnant female patients with severe COVID-19, and asymptomatic COVID-19 (see Table S4). We analyzed a total of 181,112 single cells, which grouped into the following circulating immune cell lineages: T (CD4⁺ and CD8⁺) and NK cells (95,225 cells), mononuclear phagocytic (MNP) cells (66,719 cells), and B and plasma cells (19,168 cells; Figures S6A–S6C). There were no significant differences in the abundance of these main lineages between pregnant and non-pregnant patients with COVID-19 or across COVID-19 severities (Figures S6D and S6E).

We then sub-clustered the CD8⁺ T, CD4⁺ T, B/plasma, and MNP cells independently to further define immune cell subpopulations within each lineage with greater granularity (Figures S6F–S6I, S7A, S8A, S9A, and S9B; Table S5; see STAR Methods). First, we identified 16 distinct cell subsets within the CD8⁺ T cell lineages, including an NK/NKT cell subset (NK/NKT_1), cycling NK cell subset (NK_2), naive CD8⁺ T cells (CD8T_4_naive), two CD8⁺ T cell subsets expressing cytotoxic genes GZMK and GZMH (CD8T_1_cytotoxic, CD8T_2_cytotoxic), one CD8⁺ T cell subset with gene expression suggestive of metabolic activation (CD8T_6_met_active), and three CD161-expressing CD8⁺ T cell subsets (CD8T_9_Tc17, CD8T_10, mucosal-associated invariant T cells [MAIT]). We also identified a CD8⁺ T cell subset with high expression of *CD4* and low expression of *CD8A* and *CD8B* (CD8T_3_cytotoxic_CD4) and a CD8⁺ T cell subset with a high expression of *CXCR4* and *TGFB1* (CD8T_7) (Figure 3A). The abundance of the cytotoxic population CD8T_2_cytotoxic expressing *PRF1*, *KLRD1*, and *GZMY* was significantly lower in pregnant versus non-pregnant subjects with COVID-19, as was the cell subset CD8T_9_Tc17, a *CD161*⁻, *RORC*⁻, *CXCR6*⁻, and *GZMK*-expressing CD8⁺ T cell population suggestive of a Tc17 phenotype. In contrast, in the context of COVID-19 infection, CD8T_10, a population of CD161/*KLRB1*-expressing CD8⁺ T cells with high *CXCR4* and *TNFAIP3* expression, is significantly higher in pregnant patients; MAIT cells also showed a trend of higher abundance in pregnant patients (Figures 3B, S6J, and S6K). Of note, doublets and low-quality cell subsets had been excluded from all analyses (see STAR Methods). Collectively, these shifts in cell subset abundance suggest that pregnant individuals have an altered capacity to mount specific immune responses in the setting of SARS-CoV-2 infection compared to non-pregnant individuals, and this occurs across a spectrum of mechanisms, including less robust classic cytotoxic CD8⁺ T cell (CD8T_2_cytotoxic) and mitigated Tc17 (CD8T_9_Tc17) responses.²⁷ In parallel, our data demonstrate that pregnant individuals with COVID-19 may have higher levels of other specialized *KLRB1*-expressing CD8⁺ T cell responses (CD8T_10, MAIT; Figure 3B), which have been shown to play an important role in mediating antimicrobial defense while maintaining the immune tolerance state of pregnancy.⁷⁹

Paired T cell receptor (TCR) repertoire sequencing was also profiled for each of these specimens, which were then associated with the single-cell gene expression measurements by shared cellular barcode; expanded TCR clones were defined

to have a frequency of at least 1% per sample and exist in at least five single cells. Using these parameters, we identified a total of 341 expanded clones across 10,833 single CD8⁺ T cells. Overall, the highest percentage of expanded clones were identified in the cytotoxic CD8T_2_cytotoxic, the *CD40LG*-expressing CD8T_3_cytotoxic, and NK/NKT_1 cell subsets (Figures S10A–S10D). Within the context of SARS-CoV-2 infection, the frequency of expanded clones in pregnancy was significantly higher in the CD8T_3_cytotoxic_CD4 cell subset compared to non-pregnant individuals, whereas clonal expansion of CD8 T cells occurred predominantly in CD8T_2_cytotoxic cells in non-pregnant individuals (Figures 3C, 3D, and S10E–S10G). The pregnancy-associated clonal expansion emerging from CD8T_3_cytotoxic_CD4—a subset of CD8 T cells with a distinctive transcriptional footprint characterized by low expression of *CD8A* and *CD8B* and relatively high expression of *CD4*, *CD40LG*, and *CD6* (Figures 3A and S6G)—also demonstrated cytotoxic markers shared by neighboring cell subsets (*GZMH*, *GZLY*, *FGFBP2*, *PRF1*) and concurrent expression of surface protein markers CD45RO, KLRG1, CD150 (SLAMF6), and CD57 (Figure 3E). While CD8T_3_cytotoxic_CD4 expresses cytotoxic markers, some markers such as *GZMB*, *GZMH*, and *PRF*, express significantly lower in pregnant patients with COVID compared to non-pregnant patients with COVID (Figures S6L and S6M). Lower cytotoxicity marker expression is also apparent in all CD8 T cells but to a lesser extent than CD8T_3_cytotoxic_CD4 (Figure S6N). A similar CD8 T cell type expressing CD4 and *CD40LG* was suggested to have helper functions.⁸⁰ While CD4-expressing CD8⁺ T cells have also been reported to be present in viral infections, including SARS-CoV-2,^{81,82} our data highlight the clonal expansion of this specific T cell type in pregnancy.

Using the database VDJdb,⁸³ we queried the identity of putative cognate epitopes to the TCR clones identified in our dataset and identified epitopes for 91 different clones from 810 single cells (Table S6). Clones with specificity to SARS-CoV-2 epitopes were most abundant in the Tc17-like CD8T_9 cell subset and MAIT cells (Figures 3F and 3G; Table S7). Interestingly, there is no enrichment of TCRs that putatively identify SARS-CoV-2 in CD8T_3_cytotoxic_CD4, the expanded cell subset in pregnant patients with COVID-19. Given the limited knowledge about the specific targets associated with various TCR sequences, the absence of a TCR sequence from VDJdb does not definitively preclude its capacity to recognize epitopes of the virus. That being said, we identified some TCRs with specificity to SARS-CoV-2 in other cell subsets (Figures 3F and 3G), indicating a difference in the epitopes that CD8T_3's TCRs target. While there were non-SARS-CoV-2-related epitopes identified that could putatively bind these TCR clones, no enrichment to a specific non-SARS-CoV-2 epitope was detected when the analysis was stratified to COVID-19 severity or specific CD8 T cell subsets, even while accounting for HLA alleles (see STAR Methods, Table S8). TCR diversity of CD8⁺ T cell repertoires was not significantly different between pregnant COVID-19 patients compared to non-pregnant COVID-19 patients (Figure S10H by Mann-Whitney test on $q = 0, 1, 2, 3, 4$). We did not detect expanded TCR clones in CD4⁺ T cells or expanded B cell receptor (BCR) clones in our single-cell cohort (Figures S7A, S7D–S7F, S8A, S8D–S8F). Taken together, these data demonstrate differences

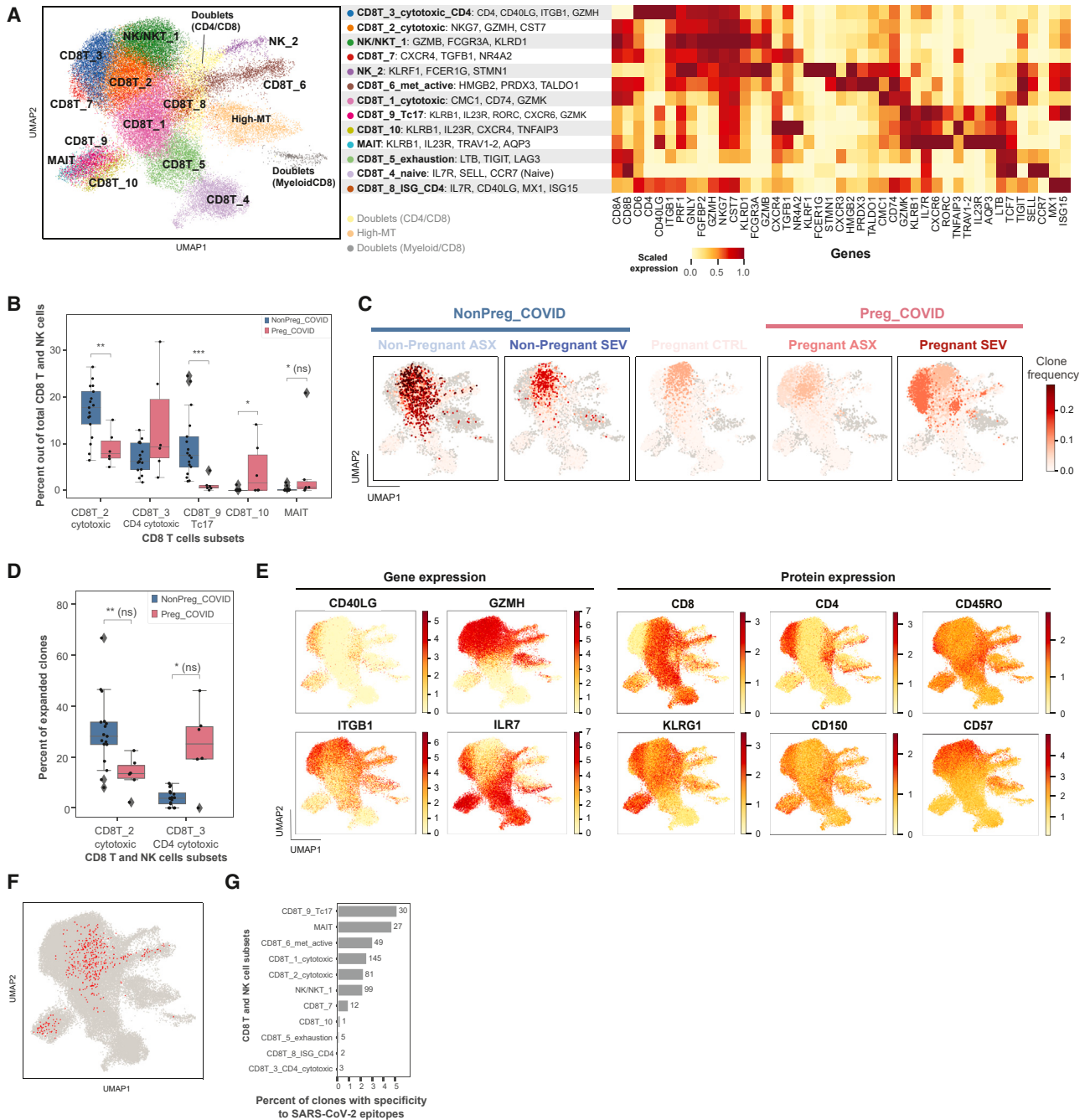


Figure 3. Changes in CD8⁺ T cell clonal expansion and cell subset abundances in pregnant patients with COVID-19

(A) Uniform manifold approximation and projection (UMAP) embedding of 50,140 CD8⁺ T and NK cells and their clustering to 13 cell subsets (left). Expression of main marker genes, scaled mean log (counts per million, CPM) (right).

(B) A boxplot illustrating the abundance of CD8⁺ T cell subsets out of all CD8⁺ T and NK cells.

(C) Frequency of TCR clones projected on CD8⁺ T and NK cell UMAP and split by condition (SEV, severe; ASX, asymptomatic; CTRL, control).

(D) A boxplot illustrating the percentage of expanded clones out of total expanded clones per cell subset in pregnant versus non-pregnant COVID-19 patients.

(E) Gene and protein expression that characterize cell subset CD8₃ cytotoxic_CD4; hex bin plots with log(CPM).

(F) TCR clones with specificity to SARS-CoV-2 projected onto CD8⁺ T and NK UMAPs.

(G) Percentage of TCR clones with specificity to SARS-CoV-2 epitopes out of total cells in each cell subset (x axis) and number of cells with SARS-CoV-2 specificity (annotation at the end of the bars). **p* < 0.05, ***p* < 0.01, ****p* < 0.001.

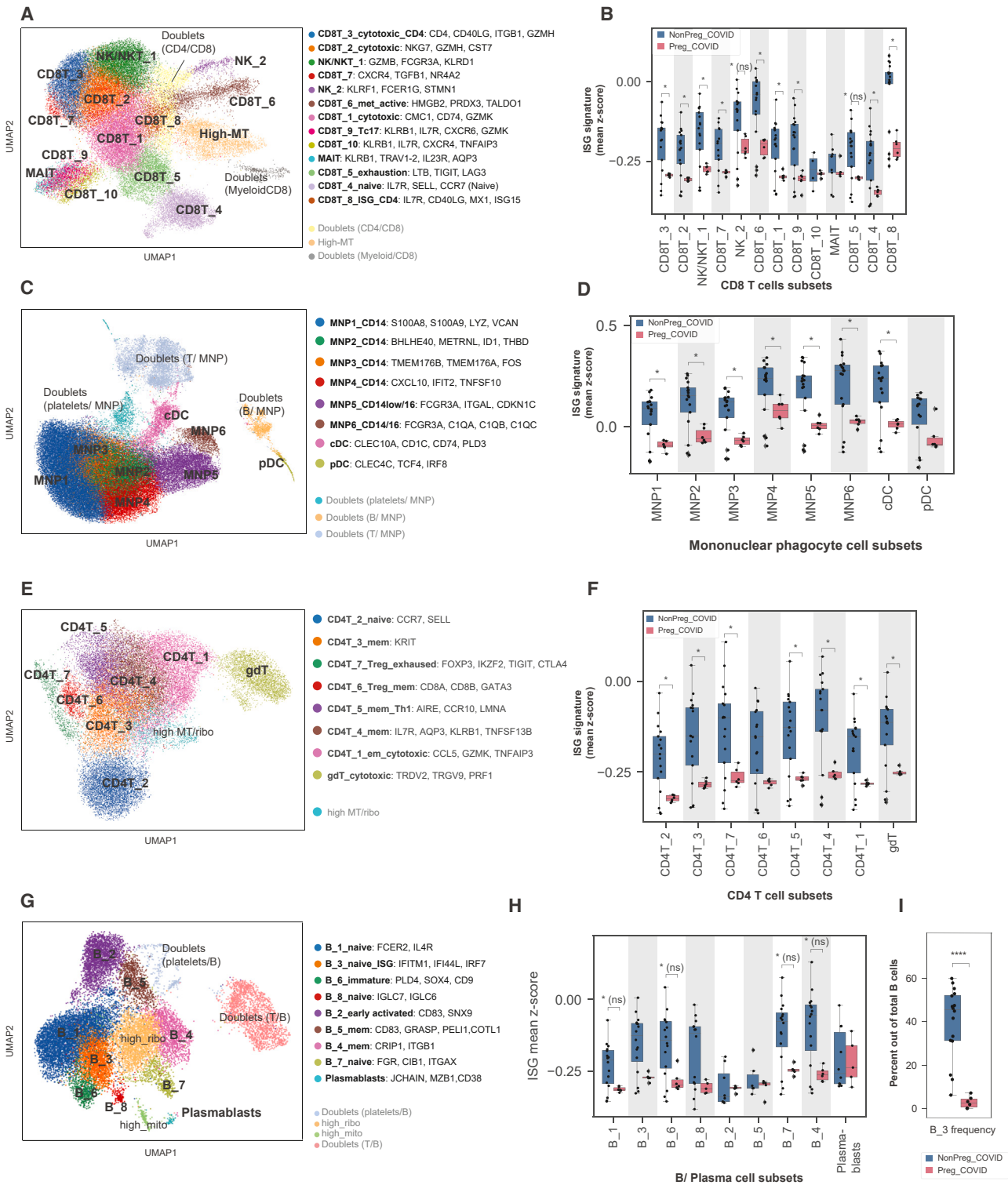


Figure 4. ISGs are downregulated in pregnant patients with COVID-19

(A) UMAP embedding of 50,140 CD8⁺ T and NK cells and their clustering to 13 cell subsets.

(B) A boxplot illustrating the expression signature of 91 ISGs across CD8⁺ T cell subsets in pregnant versus non-pregnant COVID-19 patients.

(C) UMAP embedding of 66,719 mononuclear phagocyte (MNP) cells and their clustering to eight cell subsets.

(D) A boxplot illustrating the expression signature of 91 ISGs across MNP cell subsets in pregnant versus non-pregnant COVID-19 patients.

(legend continued on next page)

in CD8⁺ T cell adaptive host immune responses, TCR clonality, diversity, and potential to bind viral epitopes in COVID-19 infection during pregnancy.

Impaired ISG expression in pregnant women

Interferon-stimulated gene (ISG) expression is a key immune response for protective SARS-CoV-2 immunity.^{84,85} However, uncontrolled ISG responses may contribute to COVID-19 severity.^{86,87} We assessed ISG expression across PBMC lineages in non-pregnant and pregnant patients with COVID-19, leveraging our scRNA-seq analyses to investigate how pregnancy influences IFN responses. Out of 270 ISGs selected as described in the STAR Methods, 91 showed a significant differential expression in at least one cell subset in pregnant vs. non-pregnant patients with COVID-19. The overall expression level of these ISGs was lower in pregnant patients with COVID-19 (Figure 4). We found decreased expression signature of 91 ISGs (see list in Table S9) in CD8⁺ T cell subsets CD8T_1, 2, 3, 4, 6, 7, 8, and 9 and NK/NKT_1 cell subsets in pregnant compared to non-pregnant individuals with COVID-19 (Figures 4A and 4B). Similar results were obtained across MNP, CD4⁺, and B cell subsets defined by scRNA-seq (Figures 4C–4H and S10I). While there was no significant difference in differential abundance in the eight MNP populations observed across either COVID-19 severity or pregnancy perturbation states (Figures S9C and S9D), in all MNP cell subsets (except pDCs)—including four CD14-high and CD16-negative cell subsets (MNP_1, MNP_2, MNP_3, and MNP_4), two cell subsets with varying expression of CD16 (MNP_5 and MNP_6), and cDCs—there was decreased expression of ISGs in pregnant compared to non-pregnant patients with COVID-19 (Figure 4D). Interestingly, similar results were also identified in CD4⁺ T cell subsets (Figure 4F). While there were no significant differences in cluster abundance across the eight CD4 T cell subsets defined by scRNA-seq analysis (Figures S7A–S7C), there was decreased expression of ISGs in all CD4-expressing populations except CD4T_6 (Figures 4E and 4F). While ISG expression was not significantly different across B cell subsets (Figures S8A–S8C, 4H), there was significantly decreased abundance of the IFITM1, IFI44L-expressing B cell subcluster 3 (B_3_naive_ISG) in pregnant compared to non-pregnant patients with COVID-19 (Figures 4G, 4I, and S8C), consistent with the theme of diminished ISG-related responses in pregnant individuals across multiple PBMC lineages. We also noted that, unlike non-pregnant individuals, plasma IFN- α 2 protein level was not increased in pregnant women even after SARS-CoV-2 infection (Figure S11), further indicating that the IFN response may be subdued in pregnancy. Reduced ISG responses in pregnant individuals with SARS-CoV-2 infection suggest a potential mechanism underlying pregnant individuals' increased susceptibility to severe viral infections.

Distinctive gut microbiota species in pregnant women with COVID-19

Recent data indicate that SARS-CoV-2 infection induces changes in the gut microbiota⁸⁸ and these changes may affect the disease course.⁸⁹ We performed shotgun metagenomic sequencing analyses with non-pregnant or pregnant women's stool samples collected from SARS-CoV-2-negative and SARS-CoV-2-infected groups. We did not find differences in alpha diversity (a measure for species richness and evenness) (Figure S12A) and beta diversity (a statistic used to quantify the compositional dissimilarity) of microbial communities from SARS-CoV-2-infected pregnant women compared to those from non-pregnant women (Figure S12B). However, by investigating species-level differences, we found that pregnant patients with COVID-19 have an increased relative abundance of *Roseburia faecis*, *Eubacterium* species CAG 38, and *Eubacterium eligens* and a decreased abundance of *Lactobacillus rhamnosus* and *Erysipelatoclostridium ramosum* compared to non-pregnant patients with COVID-19 (Figure S12C). Among SARS-CoV-2-infected pregnant women with different clinical severity, we did not observe significant differences in alpha diversity according to control or case severity categories among pregnant women (Figure S12D) and beta diversity (Figure S12E). However, when we compared the bacterial species-level differences between pregnant patients with COVID-19 to pregnant controls, we found that *Phascolarctobacterium faecium*, *Parabacteroides merdae*, *Intestinimonas butyriciproducens*, *Bacteroides fragilis*, *Asaccharobacter celatus*, *Alistipes putredinis*, and *Adlercreutzia equolifaciens* were significantly reduced in pregnant patients with COVID-19 compared to pregnant controls. In parallel, *Actinomyces graevenitzi*, a species suggested to contribute to preterm deliveries,⁹⁰ increased in its abundance (Figure S12F). These data indicate that pregnancy influences the relative abundance of certain gut bacterial species, and alterations in gut microbiota are further affected by COVID-19. Recent studies indicated that the maternal microbiota community influences the long-lasting health of offspring,^{91–93} thus warranting future studies of altered microbiota in pregnancy at baseline and upon viral infection.

Distinct cytokine and chemokine responses in non-pregnant versus pregnant patients with COVID-19

The unrestrained production of cytokines or chemokines, the “cytokine storm,” is a well-described feature in some cases of severe COVID-19.^{10,13,18,94} However, previous studies have not compared cytokine levels between non-pregnant COVID-19 and pregnant COVID-19. To gain insight into the differences in inflammatory response between pregnant and non-pregnant individuals with COVID-19, we collected plasma samples from 107 individuals, as described in Tables S1, S2, and S3, to assess the levels of 71 cytokines, chemokines, and growth factors

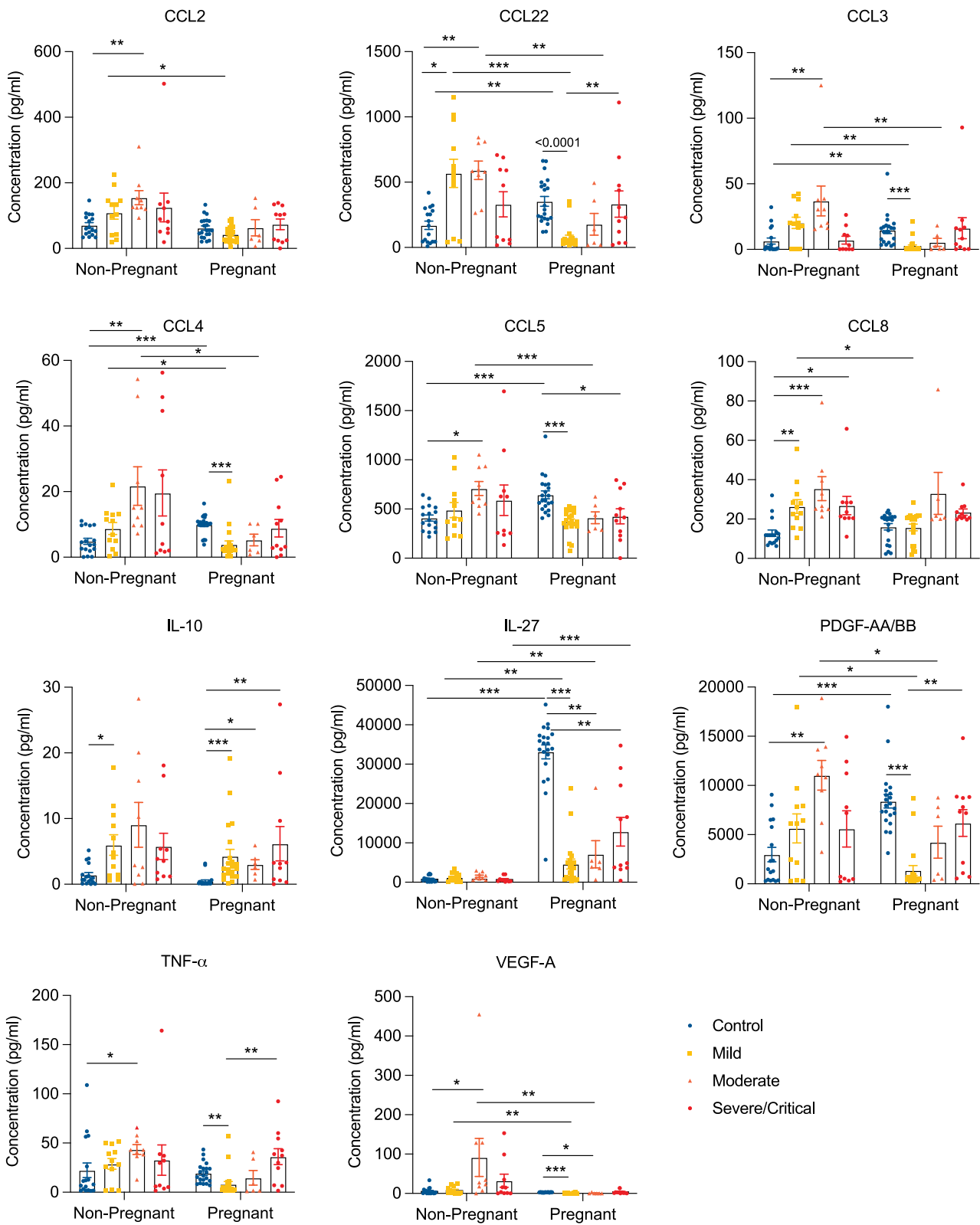
(E) UMAP embedding of 29,960 CD4⁺ T cells and their clustering to eight cell subsets.

(F) A boxplot illustrating the expression signature of 91 ISGs across CD4 T cell subsets in pregnant versus non-pregnant COVID-19 patients.

(G) UMAP embedding of 19,168 B and plasma cells and their clustering to nine cell subsets.

(H) A boxplot illustrating the expression signature of 91 ISGs across B cell subsets in pregnant versus non-pregnant COVID-19 patients.

(I) A boxplot illustrating the B_3_naive_ISG cell subset abundances in pregnant versus non-pregnant COVID-19 patients. NonPreg_COVID includes non-pregnant patients with asymptomatic and severe COVID-19; Preg_COVID includes pregnant patients with asymptomatic and severe COVID-19. **p* < 0.05, ****p* < 0.001.



(legend on next page)

(Figures 5 and S13). We found that COVID-19 disease severity^{47,48} was a key consideration in understanding cytokine elevation or suppression in the setting of acute disease. Moreover, we identified substantial differences between the pregnant and non-pregnant cytokine/chemokine and growth factor response to COVID-19, with several different patterns of cytokine expression. Among those tested, only one cytokine, IL-10, was altered similarly in pregnant and non-pregnant individuals with acute COVID-19 infection; IL-10 increased with acute infection in both groups, consistent with earlier data from non-pregnant individuals.^{10,11,14,18} In contrast, several cytokines, chemokines, and growth factors were altered by COVID-19 in opposite directions between pregnant and non-pregnant individuals, including TNF- α , VEGF-A, CCL3, CCL4, CCL22, CCL5, and PDGF-AA/BB (Figure 5); all of these were increased in acute COVID-19 in non-pregnant individuals but reduced in pregnant individuals with mild COVID-19, relative to respective uninfected control populations. A slight exception was TNF- α , which was increased in non-pregnant individuals with COVID-19 relative to uninfected controls and reduced among pregnant with mild COVID-19 but increased in pregnancy as disease severity increased. Many cytokines and chemokines were increased by pregnancy itself (Figures 5 and S16), with significantly increased levels noted in pregnant uninfected controls relative to non-pregnant uninfected (IL-27, CCL3, CCL4, CCL22, CCL5, and PDGF-AA/BB). Finally, we noted several cytokines were significantly reduced in pregnant individuals with COVID-19 relative to non-pregnant individuals with COVID-19, including CCL2, CCL8, VEGF-A, CCL-3, CCL-4, CCL-22, CCL-5, and PDGF-AA/BB. In contrast, IL-27 was the only cytokine that was significantly increased among all pregnant groups (uninfected controls and COVID-19 acute infections) relative to their non-pregnant counterparts, and significantly suppressed in COVID-19 infection among pregnant patients, relative to pregnant controls.

Taken together, these results demonstrate the impact of pregnancy on baseline levels of immune-related soluble factors, such as cytokines and chemokines, in blood circulation. Their relative abundance in non-pregnant and pregnant individuals is further shaped by viral infection, indicating a complex interplay between the host immune response associated with pregnancy and respiratory viral infection that culminated in the altered production of cytokines and chemokines in blood circulation.

High body mass index and pregnancy synergistically alter immune responses

Obesity represents the most common comorbidity during pregnancy and has been recognized as a risk factor for severe COVID-19.⁹⁵ For example, obesity-associated, chronic, low-grade inflammation and impaired lung function may underlie enhanced susceptibility to infection.⁹⁶ Thus, we sought to examine whether maternal obesity (pre-pregnancy body mass

index [BMI] ≥ 30 kg/m²) was associated with altered immune responses in pregnant patients with COVID-19 and whether obesity impacted immune responses to COVID-19 differently in pregnant versus non-pregnant populations. To do so, we grouped non-pregnant and pregnant patients with COVID-19 based on obesity status. Upon *in vitro* stimulation, CD4⁺ and CD8⁺ T cells produced higher levels of IL-2, IFN- γ , and TNF- α in pregnant individuals with obesity and COVID-19 compared to non-obese (BMI < 30 kg/m²) pregnant individuals with COVID-19 (Figures S14A and S14B). COVID-19-associated IL-4 production by CD4⁺ and CD8⁺ T cells was augmented by obesity, albeit not statistically significantly, in pregnant individuals. Thus, obesity had a more pronounced impact on enhanced T cell production of inflammatory cytokines in pregnant individuals with COVID-19 compared to non-pregnant individuals (Figures S14A and S14B). Obesity augmented IFN- α plasma levels more significantly in pregnant women with COVID-19 compared to non-pregnant women, although IFN- α levels were significantly higher in non-pregnant individuals with COVID-19 compared to pregnant, regardless of obesity status (Figure S14C). Similar trends were observed for IL-1 α and IL-17A, where obesity was associated with augmented plasma levels in pregnant women with COVID-19, although neither finding achieved statistical significance ($p = 0.07$ and $p = 0.05$, respectively; Figure S14C). Despite its suggested association with suppressed monocyte function in pregnancy,⁹⁷ in our analyses, obesity was not associated with further depression of cytokine production of the COVID-19-associated monocytes. These data suggest that obesity may increase the risk of COVID-19 in pregnant individuals by augmenting T cell inflammatory functions and that the profound suppression of monocyte function that occurs in COVID-19 may not be further augmented by obesity.

Effect of fetal sex on immune responses in pregnant patients with COVID-19

While fetal sex was recently shown to influence COVID-19-related immune responses in the placenta,²⁴ it is unknown whether it also affects maternal immune responses. We first compared T cell composition and cytokine production based on fetal sex. Overall frequencies of naive, CM, and EM CD4⁺ and CD8⁺ T cells (Figures S15A and S15B) in mothers, and maternal cytokine production by CD4⁺ T cells (Figure S15C), CD8⁺ (Figure S15D), and $\gamma\delta$ T cells (Figure S15E), were comparable regardless of fetal sex. Mothers with severe or critical COVID-19 carrying a male fetus demonstrated reduced levels of plasma IL-10, IL-1RA, and IL-27 relative to mothers carrying a female fetus, although none of these reductions achieved statistical significance (Figure S15F). Among pregnant individuals with moderate COVID-19 disease severity carrying a male fetus, we detected reduced production of IFN- λ , IFN- β , and IL-6 by CD14⁺ monocytes upon *in vitro* LPS stimulation relative to individuals

Figure 5. Comparative analyses of plasma cytokines, chemokines, and growth factors of pregnant versus non-pregnant control and COVID-19 patients

Concentrations of cytokines, chemokines, and growth factors in pregnant and non-pregnant women who were healthy (non-pregnant, $n = 17$; pregnant, $n = 21$) or who had mild (non-pregnant, $n = 12$; pregnant, $n = 21$), moderate (non-pregnant, $n = 9$; pregnant, $n = 6$), or severe/critical (non-pregnant, $n = 10$; pregnant, $n = 11$) COVID-19.

Data are shown as the mean \pm SEM. * $p < 0.05$, ** $p < 0.01$, *** $p < 0.001$.

with moderate COVID-19 carrying a female fetus (Figure S15G), although only the reduction in IFN- λ achieved statistical significance. Overall, these findings suggest that fetal sex may subtly influence maternal immune responses in the setting of SARS-CoV-2 in pregnancy, and this area is worthy of study in cohorts with larger numbers of males and females per biological group and/or a less heterogeneous viral infection phenotype.

DISCUSSION

Studies have suggested that pregnant women are at a higher risk of experiencing complications and mortality associated with SARS-CoV-2 infection.^{98–100} However, the mechanisms underlying this increased susceptibility during pregnancy are not well understood. Furthermore, conflicting findings in earlier studies, perhaps due to limitations such as small sample sizes, heterogeneous timing of sample collection, and/or lack of availability of appropriate pregnant and non-pregnant controls, posed a challenge in formulating a comprehensive understanding of the modulatory effects of pregnancy on immune responses to SARS-CoV-2 and other infections.

To gain deeper insights into how pregnancy affects host immune responses at baseline and following viral infections, we characterized samples, such as PBMCs, plasma, and the gut microbiome (stool), collected from pregnant and age-matched non-pregnant women during the acute and convalescent phases of SARS-CoV-2 infection, compared to samples from pregnant and non-pregnant SARS-CoV-2-negative controls.

Earlier work suggested that the activation of CD4⁺ and CD8⁺ T cells appears to be similar between pregnant and non-pregnant women.⁴³ In COVID-19 pregnant women, we observed impaired CD8⁺ T cell responses characterized by lower percentages of EM cells, reduced cytokine expression, reduced ISG expression, and altered clonal expansion compared to COVID-19 non-pregnant women. CD4-expressing CD8⁺ T cells in pregnant patients with COVID-19 were found to undergo a clonal expansion, while there was a clonal expansion of other cytotoxic CD8⁺ T cells in non-pregnant patients with COVID-19. Additionally, CD8⁺ T cells in infected pregnant women displayed reduced functionality, less cytokine production, and signs of T cell exhaustion. These data suggest that pregnancy-associated CD8⁺ T cells may be less equipped to combat viral infections effectively due to their higher expression of PD-1 and Tim-3, lower EM cell percentages, and altered clonal expansion. On the other hand, $\gamma\delta$ T and Th17 cell functions are elevated in mild cases of COVID-19 and infected pregnant groups, respectively, suggesting that different T cell subsets display altered functional outcomes. Additional studies will be needed to gain a mechanistic understanding of such changes. Earlier works also indicated that fetal antigen-specific CD8⁺ T cells show increased PD-1 and LAG-3 expression during secondary pregnancy.¹⁰¹ Additionally, pregnancy induces the differentiation of hypofunctional CD8⁺ T cells, which is associated with extensive epigenetic remodeling.¹⁰² These studies with murine models suggest a possible relationship between T cell exhaustion and parity. Therefore, future studies are needed to address whether parity affects T cell exhaustion in humans.

We identified decreased anti-inflammatory Treg percentages in pregnant patients with severe/critical COVID-19 compared to non-pregnant patients. Tregs are key mediators for tolerogenic responses, essential for the implantation and the maintenance of pregnancy.^{58,103} Thus, less robust Treg responses may be associated with an increased risk of developing pregnancy-associated complications, including pre-eclampsia, pre-term birth, and stillbirth.

IFN and ISG production is one of the key responses to control the disease severity of COVID-19. We found that ISG expression was generally decreased in many cell types of COVID-19 pregnant groups, which may explain why pregnant women become more susceptible to complications associated with SARS-CoV-2 infection. While an earlier study has reported impaired IFN responses during pregnancy,¹⁰⁴ our work provides extensive analyses showing the dampened IFN responses in pregnancy across many cell types. Future functional studies are warranted to understand how pregnancy affects IFN responses and whether reduced IFN responses affect the enhanced susceptibility of pregnant women to infection and inflammation.

Our scRNA-seq results showed that pregnant PBMCs include a CD4-expressing CD8⁺ T cell subset. Expansion of these double-positive cells has been observed in human^{105,106} and also reported to have antiviral capacities.¹⁰⁷ The function of these cells and their impact on antiviral immunity during pregnancy need to be studied in the future.

Impaired cytokine production by monocytes has been reported in severe cases of COVID-19.^{7,108} However, the specific functional changes in pregnant monocytes compared to non-pregnant monocytes during COVID-19 have not been well understood. We found that pregnancy is associated with enhanced monocyte function at baseline compared to non-pregnant women. Monocytes from pregnant women exhibited increased HLA-DR expression, cytokine production, and chemokine production. This enhanced monocyte activity might compensate for impaired T cell function associated with pregnancy, as monocytes play a crucial role in recruiting leukocytes to inflammatory sites through the production of chemokines, such as CCL3, CCL4, and CCL22.¹⁰⁹ Our data are consistent with other reports that monocyte function in pregnancy may be enhanced relative to the non-pregnant state.^{110,111} However, we also noted that SARS-CoV-2 infection led to long-lasting suppressive effects on monocytes that were most pronounced in pregnant women, demonstrated by reduced HLA-DR expression in intermediate and non-classical monocytes persisting into convalescence, dampened cytokine production in severe/critical disease, and reduced ISG expression in pregnant compared to non-pregnant individuals with COVID-19. In addition, given the heightened monocyte function we observed in uninfected pregnant individuals, the COVID-19-associated monocyte suppression marks an even more profound difference from the pregnant baseline state than does monocyte suppression observed in non-pregnant individuals with COVID-19.^{7,8}

Our data indicated substantial differences between the pregnant and non-pregnant cytokine/chemokine and growth factor response to COVID-19. Finally, we also demonstrated that CD4⁺ and CD8⁺ T cells from COVID-19-infected pregnant individuals with obesity produced increased cytokine levels

upon stimulation compared to non-obese pregnant individuals with COVID-19. Such interaction between obesity and COVID-19 status was not observed in non-pregnant groups. The enhanced inflammatory response may contribute to a higher risk of developing inflammatory pathologies in pregnant women with obesity.

Another important area for future study beyond the scope of the experiments performed here is to understand how maternal immune responses during acute SARS-CoV-2 infection and convalescence relate to longer-term immune function in individuals after pregnancy^{112–114} (e.g., development of long COVID or other immune syndromes) and the short- and long-term health outcomes of their offspring. Members of our study team have examined both short-term neurodevelopmental^{115,116} and cardiometabolic^{117,118} outcomes in offspring of mothers infected with SARS-CoV-2 in pregnancy, demonstrating increased risk for neurodevelopmental diagnoses at 12 months (particularly pronounced in male offspring) and increased risk for altered growth trajectories in the first year of life that may presage an increased risk for early-onset cardiometabolic complications. These follow-up studies did not link maternal immune responses 1:1 with offspring health/immune trajectories, however, and establishment of prospective cohorts to link maternal immune activation with the neurodevelopmental and cardiometabolic risk of individual offspring remains an important area for future study.

In summary, we report the most comprehensive immune survey of COVID-19 in pregnancy to date, and we identified pregnancy-specific alterations in immune responses to SARS-CoV-2, including altered T cell and monocyte function and cytokine production. Our findings of increased T cell exhaustion and profound monocyte suppression with infection in pregnancy relative to uninfected pregnant individuals, a pregnancy-specific clonal expansion of CD4-expressing CD8⁺ T cell subsets, and reduced expression of ISGs by all pregnant immune cell subsets suggest potential mechanisms by which pregnancy-specific immunity predisposes individuals to increased severity of disease with viral infection. Altogether, this work elucidates key aspects of pregnancy immunity that are important not only in understanding pregnancy-specific responses to SARS-CoV-2 but with broad implications for a better understanding of altered immunity and enhanced susceptibility to viral infection in pregnancy that can be used to guide targeted screening and therapeutic strategies in future pandemics.

Limitations of the study

There are limitations to our study. First, our COVID-19 pregnant samples were largely from third-trimester infections because these samples were collected either upon hospital admission for symptomatic COVID-19 infection (more likely for patients to have severe infection requiring hospitalization in the third trimester of pregnancy compared to first or second) or upon presentation to labor and delivery for labor or other pregnancy-related evaluation (universal SARS-CoV-2 status screening was conducted with SARS-CoV-2 nasopharyngeal PCR from April 2020 onward). Given hospital restrictions on research-only study visits at our hospitals and most across the country, it was not possible to comprehensively sample first- and

second-trimester pregnant patients for SARS-CoV-2 infection, so neither our nor any specimens banked contain a comprehensive sampling of first- and second-trimester SARS-CoV-2 infection. Given that trimester-specific immune signatures have been described,^{119,120} how SARS-CoV-2 infection in the first and second trimesters affects maternal host immune responses is a question that remains to be answered. Second, we evaluated non-specific T cell stimulation outcomes with samples collected from the acute and convalescent phases of COVID-19; we did not assess SARS-CoV-2-specific T cell responses. Third, we used LPS, instead of other Toll-like receptor (TLR) ligands, to interrogate monocyte function *in vitro*. Fourth, while we found that specific species of bacteria were altered by pregnancy and SARS-CoV-2 infection, additional studies are needed to address whether there is a causal association between bacterial composition, COVID-19 disease severity, pregnancy outcomes, and subsequent risk for offspring neurodevelopmental disorders.

RESOURCE AVAILABILITY

Lead contact

Further information and requests for resources and reagents should be directed to and will be fulfilled by the lead contact, Jun R. Huh (jun_huh@hms.harvard.edu).

Materials availability

This study did not generate new unique reagents.

Data and code availability

scRNA data, CITE-seq, and repertoire data were deposited to GEO and are available in the accession number GEO: GSE239452. The code used for single-cell analysis and figure generation is available on GitHub at https://github.com/villani-lab/COVID_pregnancy. The version used for the analyses in this study was assigned through the Zenodo repository (Zenodo: <https://doi.org/10.5281/zenodo.14014878>). A full list of software packages and versions included in the analysis can be found in [Table S12](#). Any additional information required to reanalyze the data reported in this paper is available from the [lead contact](#) upon request.

CONSORTIA

Below is the list of all MGH COVID Collection & Processing Team (Non-Pregnant Samples) participants:

Collection Team: Kendall Lavin-Parsons, Blair Parry, Brendan Lilley, Carl Lodenstein, Brenna McKaig, Nicole Charland, Hargun Khanna, and Justin Margolin.

Processing Team: Anna Gonye, Irena Gushterova, Tom Lasalle, and Nihaarika Sharma; Brian C. Russo and Maricarmen Rojas-Lopez; and Moshe Sade-Feldman, Kasidet Manakongtreecheep, Jessica Tantivit, Molly Fisher Thomas, Thomas Lasalle, and Thomas Eisenhaure.

ACKNOWLEDGMENTS

D.S.O. was supported by a postdoctoral fellowship program (Nurturing Next-generation Researchers) through the National Research Foundation of Korea (2021R1A6A3A14044062). E.K was supported by the National Research Foundation of Korea (RS-2023-00209464, RS-2023-00302229) the Technology Innovation Program (20023378) funded by the Ministry of Trade, Industry & Energy (MOTIE, South Korea) and a Korea University grant (K2225821). R.N. was supported by a postdoctoral fellowship (MGH Executive Committee on

Research Medical Discovery (FMD) Fundamental Research Fellowship Award). M.B.G., M.R.F., and N.H. were supported by an American Lung Association COVID-19 Action Initiative grant. M.B.G. and M.R.F. were supported by a grant from the Executive Committee on Research at MGH. P.S. was supported by the NHLBI K08HL157725, an American Heart Association Career Development Award, and the Brigham and Women's Hospital Innovation Evergreen Fund. O.P. and A.L. were supported by the COVID-Relief research funds from the Brigham and Women's Hospital, Department of Psychiatry. A.-C.V. acknowledges funding support from the COVID-19 Clinical Trials Pilot grant from the Executive Committee on Research at MGH, a COVID-19 Chan Zuckerberg Initiative grant (2020-216954), the funds from the Manton Foundation and the Klarman Family Foundation, and the National Institutes of Health (DP2CA247831). L.L.S. was supported by the NICHD K12HD103096. K.J.G. was supported by the NHLBI K08 HL146963 and K08 HL146963-02S1. This work was also supported by the National Institutes of Health/NICHD (R01HD100022-S2 to A.G.E.), the National Institutes of Health/NIMH (RF1MH132336 to A.G.E. and R.H.P.), Simons Foundation SFARI Maternal COVID-19 Award 870754 (to A.G.E.), and the Patricia and Scott Eston MGH Research Scholar Award, 2024-2029 (to A.G.E.). J.R.H. was supported by the Jeongho Kim Neurodevelopmental Research Fund, the N of One: Autism Research Foundation, the Simons Foundation Autism Research Initiative, and the Burroughs Wellcome Fund (the Pathogenesis of Infectious Disease Program).

AUTHOR CONTRIBUTIONS

A.G.E. and J.R.H. conceptualized the study. A.G.E. supervised all the clinical aspects of the study, metadata generation, and results interpretation. J.R.H. supervised immune analyses. A.-C.V. managed and supervised scRNA-seq data generation and analyses. D.S.O., E.K., G.L., G.B.C., A.G.E., and J.R.H. designed experiments. D.S.O., E.K., G.L., R.N., A.L., and O.P. analyzed data. MGH COVID Collection & Processing Team, P.S., J.T., A.T., and B.Y.A., collected, processed, and generated samples and/or data from the MGH acute COVID-19 non-pregnant cohort, which was overseen by X.G.Y. and J.Z.L. L.L.S., O.J., S.D., E.G., J.K., and B.A. enrolled, collected, processed, and generated samples and phenotypic data from the MGB COVID-19 Pregnancy Biorepository, which was supervised by A.G.E. and K.J.G., and to which L.Y. and A.F. also contributed personnel support and resources. M.B.G., M.R.F., and N.H. oversaw the MGH acute COVID cohort. P.S., J.T., A.T., and B.Y.A. performed the single-cell multiomics experiments for the COVID-19 pregnancy cohort. R.N. performed single-cell data analysis. R.N., P.S., and A.-C.V. performed single-cell data analysis interpretation. D.A.D. and L.H.N. performed metagenomic sequencing and analysis, supervised by A.T.C. D.S.O., E.K., G.L., R.N., P.S., A.-C.V., A.G.E., and J.R.H. wrote the manuscript. All authors read or provided comments on the manuscript.

DECLARATION OF INTERESTS

A.-C.V. has a financial interest in 10X Genomics. The company designs and manufactures gene-sequencing technology for use in research, and such technology is being used in this research. A.-C.V.'s interests were reviewed by The Massachusetts General Hospital and Mass General Brigham in accordance with their institutional policies. J.R.H. consults for CJ CheilJedang and Interon Laboratories. A.G.E. consults for Mirvie, Inc. outside of this work and receives research funding from Merck Pharmaceuticals outside of this work. K.J.G. has served as a consultant for BillionToOne, Aetion, Roche, and Janssen Global Services outside of this work.

STAR★METHODS

Detailed methods are provided in the online version of this paper and include the following:

- [KEY RESOURCES TABLE](#)
- [EXPERIMENTAL MODEL AND STUDY PARTICIPANT DETAILS](#)
 - Human participants and data collection
 - Clinical and sample definitions

METHOD DETAILS

- Blood specimen processing
- Flow cytometry-based immune cell profiling
- Monocyte enrichment and stimulation
- Cytometric bead array
- Plasma cytokine and chemokine analysis
- Single-cell cohort details
- PBMC CD45⁺ enrichment, cell hashing, CITE-seq staining
- Single-cell gene expression, feature bar code, and TCR/BCR library construction and sequencing
- scRNA-seq read alignment and quantification
- Basic and lineage-level single-cell clustering
- Single-cell subset annotation
- Single-cell differential abundance analysis
- Repertoire analysis
- Enrichment of TCR/BCR clones in cell subsets
- Putative epitopes for CD8 TCRs
- HLA alleles
- TCR sequence diversity
- ISG expression analysis
- Metagenomic analysis

QUANTIFICATION AND STATISTICAL ANALYSIS

SUPPLEMENTAL INFORMATION

Supplemental information can be found online at <https://doi.org/10.1016/j.celrep.2024.114933>.

Received: December 14, 2023

Revised: July 30, 2024

Accepted: October 16, 2024

Published: November 5, 2024

REFERENCES

1. Wu, Z., and McGoogan, J.M. (2020). Characteristics of and Important Lessons from the Coronavirus Disease 2019 (COVID-19) Outbreak in China: Summary of a Report of 72314 Cases from the Chinese Center for Disease Control and Prevention. *JAMA, J. Am. Med. Assoc.* 323, 1239–1242. <https://doi.org/10.1001/jama.2020.2648>.
2. Ye, Q., Wang, B., Mao, J., Fu, J., Shang, S., Shu, Q., and Zhang, T. (2020). Epidemiological analysis of COVID-19 and practical experience from China. *J. Med. Virol.* 92, 755–769. <https://doi.org/10.1002/jmv.25813>.
3. Zhou, P., Yang, X.L., Wang, X.G., Hu, B., Zhang, L., Zhang, W., Si, H.R., Zhu, Y., Li, B., Huang, C.L., et al. (2020). A pneumonia outbreak associated with a new coronavirus of probable bat origin. *Nature* 579, 270–273. <https://doi.org/10.1038/s41586-020-2012-7>.
4. Dong, E., Du, H., and Gardner, L. (2020). An interactive web-based dashboard to track COVID-19 in real time. *Lancet Infect. Dis.* 20, 533–534. [https://doi.org/10.1016/S1473-3099\(20\)30120-1](https://doi.org/10.1016/S1473-3099(20)30120-1).
5. Mathew, D., Giles, J.R., Baxter, A.E., Oldridge, D.A., Greenplate, A.R., Wu, J.E., Alanio, C., Kuri-Cervantes, L., Pampera, M.B., D'Andrea, K., et al. (2020). Deep immune profiling of COVID-19 patients reveals distinct immunotypes with therapeutic implications. *Science* 369, eabc8511. <https://doi.org/10.1126/SCIENCE.ABC8511>.
6. Chen, Z., and John Wherry, E. (2020). T cell responses in patients with COVID-19. *Nat. Rev. Immunol.* 20, 529–536. <https://doi.org/10.1038/s41577-020-0402-6>.
7. Schulte-Schrepping, J., Reusch, N., Paclik, D., Baßler, K., Schlickeiser, S., Zhang, B., Krämer, B., Krammer, T., Brumhard, S., Bonaguro, L., et al. (2020). Severe COVID-19 Is Marked by a Dysregulated Myeloid Cell Compartment. *Cell* 182, 1419–1440.e23. <https://doi.org/10.1016/j.cell.2020.08.001>.
8. Silvin, A., Chapuis, N., Dunsmore, G., Goubet, A.G., Dubuisson, A., Derosa, L., Almiré, C., Hénon, C., Kosmider, O., Droin, N., et al. (2020).

- Elevated Calprotectin and Abnormal Myeloid Cell Subsets Discriminate Severe from Mild COVID-19. *Cell* 182, 1401–1418.e18. <https://doi.org/10.1016/j.cell.2020.08.002>.
9. Huang, C., Wang, Y., Li, X., Ren, L., Zhao, J., Hu, Y., Zhang, L., Fan, G., Xu, J., Gu, X., et al. (2020). Clinical features of patients infected with 2019 novel coronavirus in Wuhan, China. *Lancet* 395, 497–506. [https://doi.org/10.1016/S0140-6736\(20\)30183-5](https://doi.org/10.1016/S0140-6736(20)30183-5).
 10. Yang, L., Liu, S., Liu, J., Zhang, Z., Wan, X., Huang, B., Chen, Y., and Zhang, Y. (2020). COVID-19: immunopathogenesis and Immunotherapeutics. *Signal Transduct. Targeted Ther.* 5, 128. <https://doi.org/10.1038/s41392-020-00243-2>.
 11. Blanco-Melo, D., Nilsson-Payant, B.E., Liu, W.C., Uhl, S., Hoagland, D., Moller, R., Jordan T.X., Oishi, K., Panis, M., Sachs, D., et al. (2020). Imbalanced Host Response to SARS-CoV-2 Drives Development of COVID-19. *Cell* 181, 1036–1045.e9. <https://doi.org/10.1016/j.cell.2020.04.026>.
 12. Yang, X., Yu, Y., Xu, J., Shu, H., Xia, J., Liu, H., Wu, Y., Zhang, L., Yu, Z., Fang, M., et al. (2020). Clinical course and outcomes of critically ill patients with SARS-CoV-2 pneumonia in Wuhan, China: a single-centered, retrospective, observational study. *Lancet Respir. Med.* 8, 475–481. [https://doi.org/10.1016/S2213-2600\(20\)30079-5](https://doi.org/10.1016/S2213-2600(20)30079-5).
 13. Liu, Y., Zhang, C., Huang, F., Yang, Y., Wang, F., Yuan, J., Zhang, Z., Qin, Y., Li, X., Zhao, D., et al. (2020). Elevated plasma levels of selective cytokines in COVID-19 patients reflect viral load and lung injury. *Natl. Sci. Rev.* 7, 1003–1011. <https://doi.org/10.1093/nsr/nwaa037>.
 14. Filbin, M.R., Mehta, A., Schneider, A.M., Kays, K.R., Guess, J.R., Gentili, M., Fenyves, B.G., Charland, N.C., Gonye, A.L.K., Gushterova, I., et al. (2021). Longitudinal proteomic analysis of severe COVID-19 reveals survival-associated signatures, tissue-specific cell death, and cell-cell interactions. *Cell Rep. Med.* 2, 100287. <https://doi.org/10.1016/j.xcrm.2021.100287>.
 15. Galván-Peña, S., Leon, J., Chowdhary, K., Michelson, D.A., Vijaykumar, B., Yang, L., Magnuson, A.M., Chen, F., Manickas-Hill, Z., Piechocka-Trocha, A., et al. (2021). Profound Treg perturbations correlate with COVID-19 severity. *Proc. Natl. Acad. Sci. USA* 118, e2111315118. <https://doi.org/10.1073/PNAS.2111315118>.
 16. Wang, W., Su, B., Pang, L., Qiao, L., Feng, Y., Ouyang, Y., Guo, X., Shi, H., Wei, F., Su, X., et al. (2020). High-dimensional immune profiling by mass cytometry revealed immunosuppression and dysfunction of immunity in COVID-19 patients. *Cell. Mol. Immunol.* 17, 650–652. <https://doi.org/10.1038/s41423-020-0447-2>.
 17. Rha, M.S., and Shin, E.C. (2021). Activation or exhaustion of CD8+ T cells in patients with COVID-19. *Cell. Mol. Immunol.* 18, 2325–2333. <https://doi.org/10.1038/s41423-021-00750-4>.
 18. Lucas, C., Wong, P., Klein, J., Castro, T.B.R., Silva, J., Sundaram, M., Ellingson, M.K., Mao, T., Oh, J.E., Israelow, B., et al. (2020). Longitudinal analyses reveal immunological misfiring in severe COVID-19. *Nature* 584, 463–469. <https://doi.org/10.1038/s41586-020-2588-y>.
 19. Brodin, P. (2021). Immune determinants of COVID-19 disease presentation and severity. *Nat. Med.* 27, 28–33. <https://doi.org/10.1038/s41591-020-01202-8>.
 20. Yang, L., Gou, J., Gao, J., Huang, L., Zhu, Z., Ji, S., Liu, H., Xing, L., Yao, M., and Zhang, Y. (2020). Immune characteristics of severe and critical COVID-19 patients. *Signal Transduct. Targeted Ther.* 5, 179. <https://doi.org/10.1038/s41392-020-00296-3>.
 21. Bolouri, H., Speake, C., Skibinski, D., Long, S.A., Hocking, A.M., Campbell, D.J., Hamerman, J.A., Malhotra, U., and Buckner, J.H.; Benaroya Research Institute COVID-19 Research Team (2021). The COVID-19 immune landscape is dynamically and reversibly correlated with disease severity. *J. Clin. Invest.* 131, e143648. <https://doi.org/10.1172/JCI143648>.
 22. Yu, X., Hartana, C., Srivastava, A., and Fergie, J. (2019). Immunity to SARS-CoV-2: Lessons Learned. *Front. Immunol.* 1, 654165. <https://doi.org/10.3389/fimmu.2021.654165>.
 23. Habel, J.R., Chua, B.Y., Kedzierski, L., Selva, K.J., Damelang, T., Haycroft, E.R., Nguyen, T.H., Koay, H.-F., Nicholson, S., McQuilten, H.A., et al. (2023). Immune profiling of SARS-CoV-2 infection during pregnancy reveals NK cell and $\gamma\delta$ T cell perturbations. *JCI Insight* 8, e167157. <https://doi.org/10.1172/jci.insight.167157>.
 24. Bordt, E.A., Shook, L.L., Atyeo, C., Pullen, K.M., de Guzman, R.M., Meinsohn, M.C., Chauvin, M., Fischinger, S., Yockey, L.J., James, K., et al. (2021). Maternal SARS-CoV-2 infection elicits sexually dimorphic placental immune responses. *Sci. Transl. Med.* 13, 7428. <https://doi.org/10.1126/SCITRANSLMED.AB17428>.
 25. Atyeo, C., DeRiso, E.A., Davis, C., Bordt, E.A., de Guzman, R.M., Shook, L.L., Yonker, L.M., Fasano, A., Akinwunmi, B., Lauffenburger, D.A., et al. (2021). COVID-19 mRNA vaccines drive differential antibody Fc-functional profiles in pregnant, lactating, and nonpregnant women. *Sci. Transl. Med.* 13, eabi8631. <https://doi.org/10.1126/SCITRANSLMED.AB18631>.
 26. Gee, S., Chandiramani, M., Seow, J., Pollock, E., Modestini, C., Das, A., Tree, T., Doores, K.J., Tribe, R.M., and Gibbons, D.L. (2021). The legacy of maternal SARS-CoV-2 infection on the immunology of the neonate. *Nat. Immunol.* 22, 1490–1502. <https://doi.org/10.1038/s41590-021-01049-2>.
 27. Garcia-Flores, V., Romero, R., Xu, Y., Theis, K.R., Arenas-Hernandez, M., Miller, D., Peyvandipour, A., Bhatti, G., Galaz, J., Gershater, M., et al. (2022). Maternal-fetal immune responses in pregnant women infected with SARS-CoV-2. *Nat. Commun.* 13, 320. <https://doi.org/10.1038/s41467-021-27745-z>.
 28. Pregnant and Recently Pregnant People | CDC <https://www.cdc.gov/coronavirus/2019-ncov/need-extra-precautions/pregnant-people.html>.
 29. Zambrano, L.D., Ellington, S., Strid, P., Galang, R.R., Oduyebo, T., Tong, V.T., Woodworth, K.R., Nahabedian Iii, J.F., Azziz-Baumgartner, E., Gilboa, S.M., et al. (2020). Update: Characteristics of Symptomatic Women of Reproductive Age with Laboratory-Confirmed SARS-CoV-2 Infection by Pregnancy Status — United States.
 30. Delahoy, M.J., Whitaker, M., O'Halloran, A., Chai, S.J., Kirley, P.D., Alden, N., Kawasaki, B., Meek, J., Yousey-Hindes, K., Anderson, E.J., et al. (2020). Characteristics and Maternal and Birth Outcomes of Hospitalized Pregnant Women with Laboratory-Confirmed COVID-19 — COVID-NET, 13 States, March 1–August 22, 2020. *MMWR Morb. Mortal. Wkly. Rep.* 69, 1347–1354. <https://doi.org/10.15585/MMWR.MM6938E1>.
 31. Metz, T.D., Clifton, R.G., Hughes, B.L., Sandoval, G.J., Grobman, W.A., Saade, G.R., Manuck, T.A., Longo, M., Sowles, A., Clark, K., et al. (2022). Association of SARS-CoV-2 infection with serious maternal morbidity and mortality from obstetric complications. *JAMA* 327, 748–759. <https://doi.org/10.1001/jama.2022.1190>.
 32. Villar, J., Ariff, S., Gunier, R.B., Thiruvengadam, R., Rauch, S., Kholin, A., Roggero, P., Prefumo, F., Do Vale, M.S., Cardona-Perez, J.A., et al. (2021). Maternal and Neonatal Morbidity and Mortality among Pregnant Women with and without COVID-19 Infection: The INTERCOVID Multinational Cohort Study. *JAMA Pediatr.* 175, 817–826. <https://doi.org/10.1001/jamapediatrics.2021.1050>.
 33. Ko, J.Y., DeSisto, C.L., Simeone, R.M., Ellington, S., Galang, R.R., Oduyebo, T., Gilboa, S.M., Lavery, A.M., Gundlapalli, A.V., and Shapiro-Mendoza, C.K. (2021). Adverse Pregnancy Outcomes, Maternal Complications, and Severe Illness Among US Delivery Hospitalizations With and Without a Coronavirus Disease 2019 (COVID-19) Diagnosis. *Clin. Infect. Dis.* 73, S24–S31. <https://doi.org/10.1093/cid/ciab344>.
 34. Jering, K.S., Claggett, B.L., Cunningham, J.W., Rosenthal, N., Vardeny, O., Greene, M.F., and Solomon, S.D. (2021). Clinical Characteristics and Outcomes of Hospitalized Women Giving Birth With and Without COVID-19. *JAMA Intern. Med.* 171, 714–717. <https://doi.org/10.1001/jamainternmed.2020.9241>.
 35. Abu-Raya, B., Michalski, C., Sadarangani, M., and Lavoie, P.M. (2020). Maternal Immunological Adaptation During Normal Pregnancy. *Front. Immunol.* 11, 575197. <https://doi.org/10.3389/fimmu.2020.575197>.

36. Shook, L.L., Fourman, L.T., and Edlow, A.G. (2022). Immune Responses to SARS-CoV-2 in Pregnancy: Implications for the Health of the Next Generation. *J. Immunol.* 209, 1465–1473. <https://doi.org/10.4049/JIMMUNOL.2200414>.
37. Mor, G., and Cardenas, I. (2010). The Immune System in Pregnancy: A Unique Complexity. *Am. J. Reprod. Immunol.* 63, 425–433. <https://doi.org/10.1111/j.1600-0897.2010.00836.x>.
38. Orefice, R. (2021). Immunology and the immunological response in pregnancy. *Best Pract. Res. Clin. Obstet. Gynaecol.* 76, 3–12. <https://doi.org/10.1016/j.bpobgyn.2020.07.013>.
39. Li, X., Zhou, J., Fang, M., and Yu, B. (2020). Pregnancy immune tolerance at the maternal-fetal interface. *Int. Rev. Immunol.* 39, 247–263. <https://doi.org/10.1080/08830185.2020.1777292>.
40. Chen, G., Liao, Q., Ai, J., Yang, B., Bai, H., Chen, J., Liu, F., Cao, Y., Liu, H., and Li, K. (2021). Immune Response to COVID-19 During Pregnancy. *Front. Immunol.* 12, 675476. <https://doi.org/10.3389/fimmu.2021.675476>.
41. Hanna, N., Hanna, M., and Sharma, S. (2020). Is pregnancy an immunological contributor to severe or controlled COVID-19 disease? *Am. J. Reprod. Immunol.* 84, e13317. <https://doi.org/10.1111/AJI.13317>.
42. Chen, G., Liao, Q., Ai, J., Yang, B., Bai, H., Chen, J., Liu, F., Cao, Y., Liu, H., and Li, K. (2021). Immune Response to COVID-19 During Pregnancy. *Front. Immunol.* 12, 675476. <https://doi.org/10.3389/fimmu.2021.675476>.
43. Chen, G., Zhang, Y., Zhang, Y., Ai, J., Yang, B., Cui, M., Liao, Q., Chen, H., Bai, H., Shang, D., et al. (2021). Differential immune responses in pregnant patients recovered from COVID-19. *Signal Transduct. Targeted Ther.* 6, 289. <https://doi.org/10.1038/s41392-021-00703-3>.
44. Zhao, S., Xie, T., Shen, L., Liu, H., Wang, L., Ma, X., Wu, J., Yuan, S., Mor, G., and Liao, A. (2021). An Immunological Perspective: What Happened to Pregnant Women After Recovering From COVID-19? *Front. Immunol.* 12, 631044. <https://doi.org/10.3389/fimmu.2021.631044>.
45. Cébulo-Vázquez, A., García-Espinosa, M., Briones-Garduño, J.C., Ariaga-Pizano, L., Ferat-Osorio, E., Zavala-Barrios, B., Cabrera-Rivera, G.L., Miranda-Cruz, P., García De La Rosa, M.T., Prieto-Chávez, J.L., et al. (2022). The percentage of CD39+ monocytes is higher in pregnant COVID-19+ patients than in nonpregnant COVID-19+ patients. *PLoS One* 17, e0264566. <https://doi.org/10.1371/journal.pone.0264566>.
46. Sureshchandra, S., Zulu, M.Z., Doratt, B., Jankeel, A., Tifrea, D., Edwards, R., Rincon, M., Marshall, N.E., and Messaoudi, I. (2021). Deep immune profiling of the maternal-fetal interface with mild SARS-CoV-2 infection. Preprint at bioRxiv. <https://doi.org/10.1101/2021.08.23.457408>.
47. Vaught, J., and Miller, E. Society for Maternal-Fetal Medicine Management Considerations for Pregnant Patients With COVID-19 Developed with guidance from Torre Halscott.
48. COVID-19 Treatment Guidelines Panel (2019). Coronavirus Disease 2019 (COVID-19) Treatment Guidelines (National Institutes of Health). <https://www.covid19treatmentguidelines.nih.gov/>.
49. Rios-Navarro, C., Dios, E.d., Forteza, M.J., and Bodi, V. (2021). Unraveling the thread of uncontrolled immune response in COVID-19 and stemi: An emerging need for knowledge sharing. *Am. J. Physiol. Heart Circ. Physiol.* 320, H2240–H2254. <https://doi.org/10.1152/AJPHEART.00934.2020>.
50. Richardson, S., Hirsch, J.S., Narasimhan, M., Crawford, J.M., McGinn, T., Davidson, K.W., Barnaby, D.P., Becker, L.B., Chelico, J.D., et al.; the Northwell COVID-19 Research Consortium (2020). Presenting Characteristics, Comorbidities, and Outcomes Among 5700 Patients Hospitalized With COVID-19 in the New York City Area. *JAMA* 323, 2052–2059. <https://doi.org/10.1001/JAMA.2020.6775>.
51. Zhou, F., Yu, T., Du, R., Fan, G., Liu, Y., Liu, Z., Xiang, J., Wang, Y., Song, B., Gu, X., et al. (2020). Clinical course and risk factors for mortality of adult inpatients with COVID-19 in Wuhan, China: a retrospective cohort study. *Lancet* 395, 1054–1062. [https://doi.org/10.1016/S0140-6736\(20\)30566-3](https://doi.org/10.1016/S0140-6736(20)30566-3).
52. Basheer, M., Saad, E., Hagai, R., and Assy, N. (2021). Clinical Predictors of Mortality and Critical Illness in Patients with COVID-19 Pneumonia. *Metabolites* 11. <https://doi.org/10.3390/METABO11100679>.
53. Montazersaheb, S., Hosseiniyan Khatibi, S.M., Hejazi, M.S., Tarhriz, V., Farjami, A., Ghasemian Sorbeni, F., Farahzadi, R., and Ghasemnejad, T. (2022). COVID-19 infection: an overview on cytokine storm and related interventions. *Viol. J.* 19, 92. <https://doi.org/10.1186/S12985-022-01814-1>.
54. Perreau, M., Suffiotti, M., Marques-Vidal, P., Wiedemann, A., Levy, Y., Laouénan, C., Ghosn, J., Fenwick, C., Comte, D., Roger, T., et al. (2021). The cytokines HGF and CXCL13 predict the severity and the mortality in COVID-19 patients. *Nat. Commun.* 12, 4888. <https://doi.org/10.1038/s41467-021-25191-5>.
55. Galván-Peña, S., Leon, J., Chowdhary, K., Michelson, D.A., Vijaykumar, B., Yang, L., Magnuson, A.M., Chen, F., Manickas-Hill, Z., Piechocka-Trocha, A., et al. (2021). Profound Treg perturbations correlate with COVID-19 severity. *Proc. Natl. Acad. Sci. USA* 118, e2111315118. <https://doi.org/10.1073/pnas.2111315118>.
56. Zenclussen, A.C. (2013). Adaptive Immune Responses During Pregnancy. *Am. J. Reprod. Immunol.* 69, 291–303. <https://doi.org/10.1111/AJI.12097>.
57. Kahn, D.A., and Baltimore, D. (2010). Pregnancy induces a fetal antigen-specific maternal T regulatory cell response that contributes to tolerance. *Proc. Natl. Acad. Sci. USA* 107, 9299–9304. <https://doi.org/10.1073/pnas.1003909107>.
58. Huang, N., Chi, H., and Qiao, J. (2020). Role of Regulatory T Cells in Regulating Fetal-Maternal Immune Tolerance in Healthy Pregnancies and Reproductive Diseases. *Front. Immunol.* 11, 1023–1116. <https://doi.org/10.3389/fimmu.2020.01023>.
59. Green, S., Politis, M., Rallis, K.S., Saenz de Villaverde Cortabarría, A., Efthymiou, A., Mureanu, N., Dalrymple, K.V., Scotta, C., Lombardi, G., Tribe, R.M., et al. (2021). Regulatory T Cells in Pregnancy Adverse Outcomes: A Systematic Review and Meta-Analysis. *Front. Immunol.* 12, 737862. <https://doi.org/10.3389/fimmu.2021.737862>.
60. Robertson, S.A., Prins, J.R., Sharkey, D.J., and Moldenhauer, L.M. (2013). Seminal Fluid and the Generation of Regulatory T Cells for Embryo Implantation. *Am. J. Reprod. Immunol.* 69, 315–330. <https://doi.org/10.1111/AJI.12107>.
61. Sasaki, Y., Sakai, M., Miyazaki, S., Higuma, S., Shiozaki, A., and Saito, S. (2004). Decidual and peripheral blood CD4+CD25+ regulatory T cells in early pregnancy subjects and spontaneous abortion cases. *Mol. Hum. Reprod.* 10, 347–353. <https://doi.org/10.1093/MOLEHR/GAH044>.
62. Morrissey, S.M., Geller, A.E., Hu, X., Tieri, D., Ding, C., Klaes, C.K., Cooke, E.A., Woeste, M.R., Martin, Z.C., Chen, O., et al. (2021). A specific low-density neutrophil population correlates with hypercoagulation and disease severity in hospitalized COVID-19 patients. *JCI Insight* 6. <https://doi.org/10.1172/jci.insight.148435>.
63. Lourda, M., Dzidic, M., Hertwig, L., Bergsten, H., Palma Medina, L.M., Sinha, I., Kvedaraitė, E., Chen, P., Muvva, J.R., Gorin, J.B., et al. (2021). High-dimensional profiling reveals phenotypic heterogeneity and disease-specific alterations of granulocytes in COVID-19. *Proc. Natl. Acad. Sci. USA* 118, e2109123118. <https://doi.org/10.1073/PNAS.2109123118>.
64. LaSalle, T.J., Gonye, A.L.K., Freeman, S.S., Kaplonek, P., Gushterova, I., Kays, K.R., Manakongtreecheep, K., Tantivit, J., Rojas-Lopez, M., Russo, B.C., et al. (2022). Longitudinal characterization of circulating neutrophils uncovers phenotypes associated with severity in hospitalized COVID-19 patients. *Cell Rep. Med.* 3, 100779. <https://doi.org/10.1016/J.XCRM.2022.100779>.
65. Mincheva-Nilsson, L. (2003). Pregnancy and gamma/delta T cells: Taking on the hard questions. *Reprod. Biol. Endocrinol.* 1, 120. <https://doi.org/10.1186/1477-7827-1-120>.

66. Laing, A.G., Lorenc, A., del Molino del Barrio, I., Das, A., Fish, M., Monin, L., Muñoz-Ruiz, M., McKenzie, D.R., Hayday, T.S., Francos-Quijorna, I., et al. (2020). A dynamic COVID-19 immune signature includes associations with poor prognosis. *Nat. Med.* 26, 1623–1635. <https://doi.org/10.1038/s41591-020-1038-6>.
67. Noh, J.Y., Jeong, H.W., Kim, J.H., and Shin, E.C. (2021). T cell-oriented strategies for controlling the COVID-19 pandemic. *Nat. Rev. Immunol.* 21, 687–688. <https://doi.org/10.1038/s41577-021-00625-9>.
68. Jarjour, N.N., Masopust, D., and Jameson, S.C. (2021). T Cell Memory: Understanding COVID-19. *Immunity* 54, 14–18. <https://doi.org/10.1016/j.immuni.2020.12.009>.
69. Wilk, A.J., Rustagi, A., Zhao, N.Q., Roque, J., Martínez-Colón, G.J., McKechnie, J.L., Ivison, G.T., Ranganath, T., Vergara, R., Hollis, T., et al. (2020). A single-cell atlas of the peripheral immune response in patients with severe COVID-19. *Nat. Med.* 26, 1070–1076. <https://doi.org/10.1038/s41591-020-0944-y>.
70. Wang, S.C., Li, Y.H., Piao, H.L., Hong, X.W., Zhang, D., Xu, Y.Y., Tao, Y., Wang, Y., Yuan, M.M., Li, D.J., and Du, M.R. (2015). PD-1 and Tim-3 pathways are associated with regulatory CD8+ T-cell function in decidua and maintenance of normal pregnancy. *Cell Death Dis.* 6, e1738. <https://doi.org/10.1038/cddis.2015.112>.
71. Mandal, M., Marzouk, A.C., Donnelly, R., and Ponzio, N.M. (2011). Maternal immune stimulation during pregnancy affects adaptive immunity in offspring to promote development of TH17 cells. *Brain Behav. Immun.* 25, 863–871. <https://doi.org/10.1016/j.bbi.2010.09.011>.
72. Choi, G.B., Yim, Y.S., Wong, H., Kim, S., Kim, H., Kim, S.V., Hoeffer, C.A., Littman, D.R., and Huh, J.R. (2016). The maternal interleukin-17a pathway in mice promotes autism-like phenotypes in offspring. *Science* 357, 933–939. <https://doi.org/10.1126/SCIENCE.AAD0314>.
73. Kim, S., Kim, H., Yim, Y.S., Ha, S., Atarashi, K., Tan, T.G., Longman, R.S., Honda, K., Littman, D.R., Choi, G.B., and Huh, J.R. (2017). Maternal gut bacteria promote neurodevelopmental abnormalities in mouse offspring. *Nature* 549, 528–532. <https://doi.org/10.1038/nature23910>.
74. Zawada, A.M., Rogacev, K.S., Rotter, B., Winter, P., Marell, R.R., Fliser, D., and Heine, G.H. (2011). SuperSAGE evidence for CD14 ++CD16 + monocytes as a third monocyte subset. *Blood* 118, 50–61. <https://doi.org/10.1182/blood-2011-01-326827>.
75. Ziegler-Heitbrock, L., Ancuta, P., Crowe, S., Dalod, M., Grau, V., Hart, D.N., Leenen, P.J.M., Liu, Y.J., MacPherson, G., Randolph, G.J., et al. (2010). Nomenclature of monocytes and dendritic cells in blood. *Blood* 116, e74–e80. <https://doi.org/10.1182/blood-2010-02-258558>.
76. Payen, D., Cravat, M., Maadadi, H., Didelot, C., Prosic, L., Dupuis, C., Losser, M.R., and De Carvalho Bittencourt, M. (2020). A Longitudinal Study of Immune Cells in Severe COVID-19 Patients. *Front. Immunol.* 11, 580250. <https://doi.org/10.3389/fimmu.2020.580250>.
77. Giamarellos-Bourboulis, E.J., Netea, M.G., Rovina, N., Akinosoglou, K., Antoniadou, A., Antonakos, N., Damoraki, G., Gkavogianni, T., Adami, M.E., Katsaounou, P., et al. (2020). Complex Immune Dysregulation in COVID-19 Patients with Severe Respiratory Failure. *Cell Host Microbe* 27, 992–1000.e3. <https://doi.org/10.1016/j.chom.2020.04.009>.
78. Spinetti, T., Hirzel, C., Fux, M., Walti, L.N., Schober, P., Stueber, F., Luedi, M.M., and Schefold, J.C. (2020). Reduced Monocytic Human Leukocyte Antigen-DR Expression Indicates Immunosuppression in Critically Ill COVID-19 Patients. *Anesth. Analg.* 131, 993–999. <https://doi.org/10.1213/ANE.0000000000005044>.
79. Raffetseder, J., Lindau, R., van der Veen, S., Berg, G., Larsson, M., and Ernerudh, J. (2021). MAIT Cells Balance the Requirements for Immune Tolerance and Anti-Microbial Defense During Pregnancy. *Front. Immunol.* 12, 718168. <https://doi.org/10.3389/FIMMU.2021.718168>.
80. Frensch, M., Stark, R., Matzmohr, N., Meier, S., Durlanik, S., Schulz, A.R., Stervbo, U., Jürchott, K., Gebhardt, F., Heine, G., et al. (2013). CD40L expression permits CD8+ T cells to execute immunologic helper functions. *Blood* 122, 405–412. <https://doi.org/10.1182/BLOOD-2013-02-483586>.
81. Meckliff, B.J., Ramírez-Suástegui, C., Fajardo, V., Chee, S.J., Kusnadi, A., Simon, H., Eschweiler, S., Grifoni, A., Pelosi, E., Weiskopf, D., et al. (2020). Imbalance of Regulatory and Cytotoxic SARS-CoV-2-Reactive CD4+ T Cells in COVID-19. *Cell* 183, 1340–1353.e16. <https://doi.org/10.1016/J.CELL.2020.10.001>.
82. Cenerenti, M., Saillard, M., Romero, P., and Jandus, C. (2022). The Era of Cytotoxic CD4 T Cells. *Front. Immunol.* 13, 867189. <https://doi.org/10.3389/fimmu.2022.867189>.
83. Shugay, M., Bagaev, D.V., Zvyagin, I.V., Vroomans, R.M., Crawford, J.C., Dolton, G., Komech, E.A., Sycheva, A.L., Koneva, A.E., Egorov, E.S., et al. (2018). VDJdb: a curated database of T-cell receptor sequences with known antigen specificity. *Nucleic Acids Res.* 46, D419–D427. <https://doi.org/10.1093/NAR/GKX760>.
84. Lee, J.S., and Shin, E.C. (2020). The type I interferon response in COVID-19: implications for treatment. *Nat. Rev. Immunol.* 20, 585–586. <https://doi.org/10.1038/s41577-020-00429-3>.
85. Diamond, M.S., and Kanneganti, T.D. (2022). Innate immunity: the first line of defense against SARS-CoV-2. *Nat. Immunol.* 23, 165–176. <https://doi.org/10.1038/s41590-021-01091-0>.
86. Lucas, C., Wong, P., Klein, J., Castro, T.B.R., Silva, J., Sundaram, M., Ellingson, M.K., Mao, T., Oh, J.E., Israelow, B., et al. (2020). Longitudinal analyses reveal immunological misfiring in severe COVID-19. *Nature* 584, 463–469. <https://doi.org/10.1038/s41586-020-2588-y>.
87. Lee, J.S., Park, S., Jeong, H.W., Ahn, J.Y., Choi, S.J., Lee, H., Choi, B., Nam, S.K., Sa, M., Kwon, J.S., et al. (2020). Immunophenotyping of covid-19 and influenza highlights the role of type I interferons in development of severe covid-19. *Sci. Immunol.* 5, 1554. <https://doi.org/10.1126/sciimmunol.abd1554>.
88. Wang, B., Zhang, L., Wang, Y., Dai, T., Qin, Z., Zhou, F., and Zhang, L. (2022). Alterations in microbiota of patients with COVID-19: potential mechanisms and therapeutic interventions. *Signal Transduct. Targeted Ther.* 7, 143. <https://doi.org/10.1038/s41392-022-00986-0>.
89. Lai, P., Nguyen, L., Okin, D., Drew, D., Battista, V., Jesudasan, S., Kuntz, T., Bhosle, A., Thompson, K., Reinicke, T., et al. (2022). Metagenomic Assessment of Gut Microbial Communities and Risk of Severe COVID-19 (ResearchSquare). <https://doi.org/10.21203/RS.3.RS-1717624/V1>.
90. Estrada, S.M., Magann, E.F., and Napolitano, P.G. (2017). Actinomyces in pregnancy: a review of the literature. *Obstet. Gynecol. Surv.* 72, 242–247. <https://doi.org/10.1097/OGX.0000000000000423>.
91. Kim, E., Paik, D., Ramirez, R.N., Biggs, D.G., Park, Y., Kwon, H.K., Choi, G.B., and Huh, J.R. (2022). Maternal gut bacteria drive intestinal inflammation in offspring with neurodevelopmental disorders by altering the chromatin landscape of CD4+ T cells. *Immunity* 55, 145–158.e7. <https://doi.org/10.1016/j.immuni.2021.11.005>.
92. Sikder, M.A.A., Rashid, R.B., Ahmed, T., Sebina, I., Howard, D.R., Ullah, M.A., Rahman, M.M., Lynch, J.P., Curren, B., Werder, R.B., et al. (2023). Maternal diet modulates the infant microbiome and intestinal Flt3L necessary for dendritic cell development and immunity to respiratory infection, 56, pp. 1098–1114.e10. <https://doi.org/10.1016/j.immuni.2023.03.002>.
93. Kimura, I., Miyamoto, J., Ohue-Kitano, R., Watanabe, K., Yamada, T., Onuki, M., Aoki, R., Isobe, Y., Kashiwara, D., Inoue, D., et al. (2020). Maternal gut microbiota in pregnancy influences offspring metabolic phenotype in mice. *Science* 367, eaaw8429. <https://doi.org/10.1126/science.aaw8429>.
94. Metzemaekers, M., Vanheule, V., Janssens, R., Struyf, S., and Proost, P. (2017). Overview of the mechanisms that may contribute to the non-redundant activities of interferon-inducible CXC chemokine receptor 3 ligands. *Front. Immunol.* 8, 1970. <https://doi.org/10.3389/fimmu.2017.01970>.
95. Kompaniyets, L., Goodman, A.B., Belay, B., Freedman, D.S., Sucusky, M.S., Lange, S.J., Gundlapalli, A.V., Boehmer, T.K., and Blanck, H.M. (2021). Body Mass Index and Risk for COVID-19-Related Hospitalization, Intensive Care Unit Admission, Invasive Mechanical Ventilation, and

- Death — United States, March–December 2020. *MMWR Morb. Mortal. Wkly. Rep.* 70, 355–361. <https://doi.org/10.15585/mmwr.mm7010e4>.
96. Popkin, B.M., Du, S., Green, W.D., Beck, M.A., Algaith, T., Herbst, C.H., Alsukait, R.F., Alluhidan, M., Alazemi, N., and Shekar, M. (2020). Individuals with obesity and COVID-19: A global perspective on the epidemiology and biological relationships. *Obes. Rev.* 21, e13128. <https://doi.org/10.1111/obr.13128>.
97. Sureshchandra, S., Marshall, N.E., Mendoza, N., Jankeel, A., Zulu, M.Z., and Messaoudi, I. (2021). Functional and genomic adaptations of blood monocytes to pregravid obesity during pregnancy. *iScience* 24, 102690. <https://doi.org/10.1016/J.ISCI.2021.102690>.
98. McClymont, E., Albert, A.Y., Alton, G.D., Boucoiran, I., Castillo, E., Fell, D.B., Kuret, V., Poliquin, V., Reeve, T., Scott, H., et al. (2022). Association of SARS-CoV-2 Infection During Pregnancy With Maternal and Perinatal Outcomes. *JAMA* 327, 1983–1991. <https://doi.org/10.1001/jama.2022.5906>.
99. Schwartz, D.A., Mulkey, S.B., and Roberts, D.J. (2023). SARS-CoV-2 placentitis, stillbirth, and maternal COVID-19 vaccination: clinical–pathologic correlations. *Am. J. Obstet. Gynecol.* 228, 261–269. <https://doi.org/10.1016/j.ajog.2022.10.001>.
100. Male, V. (2022). SARS-CoV-2 infection and COVID-19 vaccination in pregnancy. *Nat. Rev. Immunol.* 22, 277–282. <https://doi.org/10.1038/s41577-022-00703-6>.
101. Kinder, J.M., Turner, L.H., Stelzer, I.A., Miller-Handley, H., Burg, A., Shao, T.Y., Pham, G., and Way, S.S. (2020). CD8+ T cell functional exhaustion overrides pregnancy-induced fetal antigen alloimmunization. *Cell Rep.* 31, 107784. <https://doi.org/10.1016/J.CELREP.2020.107784>.
102. Pollard, J.M., Hynes, G., Yin, D., Mandal, M., Gounari, F., Alegre, M.-L., and Chong, A.S. (2024). Pregnancy differentiates memory CD8+ T cells into hypofunctional cells with exhaustion-enriched programs. *JCI Insight* 9, e176381. <https://doi.org/10.1172/JCI.INSIGHT.176381>.
103. Samstein, R.M., Josefowicz, S.Z., Arvey, A., Treuting, P.M., and Rudensky, A.Y. (2012). Extrathymic Generation of Regulatory T Cells in Placental Mammals Mitigates Maternal-Fetal Conflict. *Cell* 150, 29–38. <https://doi.org/10.1016/J.CELL.2012.05.031>.
104. Forbes, R.L., Gibson, P.G., Murphy, V.E., and Wark, P.A.B. (2012). Impaired type I and III interferon response to rhinovirus infection during pregnancy and asthma. *Thorax* 67, 209–214. <https://doi.org/10.1136/THORAXJNL-2011-200708>.
105. Weiss, L., Roux, A., Garcia, S., Demouchy, C., Haefner-Cavaillon, N., Kazatchkine, M.D., and Gougeon, M.L. (1998). Persistent expansion, in a human immunodeficiency virus-infected person, of β -restricted CD4+ CD8+ T lymphocytes that express cytotoxicity-associated molecules and are committed to produce interferon- γ and tumor necrosis factor- α . *J. Infect. Dis.* 178, 1158–1162. <https://doi.org/10.1086/515674>.
106. Frahm, M.A., Picking, R.A., Kuruc, J.D., McGee, K.S., Gay, C.L., Eron, J.J., Hicks, C.B., Tomaras, G.D., and Ferrari, G. (2012). CD4+CD8+ T Cells Represent a Significant Portion of the Anti-HIV T Cell Response to Acute HIV Infection. *J. Immunol.* 188, 4289–4296. <https://doi.org/10.4049/JIMMUNOL.1103701>.
107. Nascimbeni, M., Shin, E.C., Chiriboga, L., Kleiner, D.E., and Rehermann, B. (2004). Peripheral CD4+CD8+ T cells are differentiated effector memory cells with antiviral functions. *Blood* 104, 478–486. <https://doi.org/10.1182/BLOOD-2003-12-4395>.
108. Brauns, E., Azouz, A., Grimaldi, D., Xiao, H., Thomas, S., Nguyen, M., Ollslagers, V., Vu Duc, I., Orte Cano, C., and Del Marmol, V. (2022). Functional reprogramming of monocytes in patients with acute and convalescent severe COVID-19. <https://doi.org/10.1172/jci.insight.154183>.
109. Fajgenbaum, D.C., and June, C.H. (2020). Cytokine Storm. *N. Engl. J. Med.* 383, 2255–2273. <https://doi.org/10.1056/NEJMr2026131>.
110. Sacks, G.P., Studena, K., Sargent, K., and Redman, C.W. (1998). Normal pregnancy and preeclampsia both produce inflammatory changes in peripheral blood leukocytes akin to those of sepsis. *Am. J. Obstet. Gynecol.* 179, 80–86. [https://doi.org/10.1016/S0002-9378\(98\)70254-6](https://doi.org/10.1016/S0002-9378(98)70254-6).
111. Luppi, P., Haluszczak, C., Trucco, M., and Deloia, J.A. (2002). Normal pregnancy is associated with peripheral leukocyte activation. *Am. J. Reprod. Immunol.* 47, 72–81. <https://doi.org/10.1034/j.1600-0897.2002.10041.x>.
112. Vázquez-González, J., Fernandez-Naranjo, R., Izquierdo-Condoy, J.S., Delgado-Moreira, K., Cordovez, S., Tello-De-la-Torre, A., Paz, C., Castillo, D., Izquierdo-Condoy, N., Carrington, S.J., and Ortiz-Prado, E. (2023). Comparative analysis of long-term self-reported COVID-19 symptoms among pregnant women. *J. Infect. Public Health* 16, 430–440. <https://doi.org/10.1016/J.JIPH.2023.01.012>.
113. Afshar, Y., Gaw, S.L., Flaherman, V.J., Chambers, B.D., Krakow, D., Berghella, V., Shamshirsaz, A.A., Boatman, A.A., Aldrovandi, G., Greiner, A., et al. (2020). Clinical Presentation of Coronavirus Disease 2019 (COVID-19) in Pregnant and Recently Pregnant People. *Obstet. Gynecol.* 136, 1117–1125. <https://doi.org/10.1097/AOG.0000000000004178>.
114. Santos, C.A.D., Fonseca Filho, G.G., Alves, M.M., Macedo, E.Y.L., Pontes, M.G.d.A., Paula, A.P., Barreto, C.T.R., Zeneide, F.N., Nery, A.F., Freitas, R.A.O., and D'Souza-Li, L. (2022). Maternal and Neonatal Outcomes Associated with Mild COVID-19 Infection in an Obstetric Cohort in Brazil. *Am. J. Trop. Med. Hyg.* 107, 1060–1065. <https://doi.org/10.4269/AJTMH.22-0421>.
115. Edlow, A.G., Castro, V.M., Shook, L.L., Haneuse, S., Kaimal, A.J., and Perlis, R.H. (2023). Sex-Specific Neurodevelopmental Outcomes Among Offspring of Mothers With SARS-CoV-2 Infection During Pregnancy. *JAMA Netw. Open* 6, e234415. <https://doi.org/10.1001/JAMANETWORKOPEN.2023.4415>.
116. Edlow, A.G., Castro, V.M., Shook, L.L., Kaimal, A.J., and Perlis, R.H. (2022). Neurodevelopmental Outcomes at 1 Year in Infants of Mothers Who Tested Positive for SARS-CoV-2 During Pregnancy. *JAMA Netw. Open* 5, e2215787. <https://doi.org/10.1001/JAMANETWORKOPEN.2022.15787>.
117. Shook, L.L., Castro, V.M., Herzberg, E.M., Fourman, L.T., Kaimal, A.J., Perlis, R.H., and Edlow, A.G. (2023). Offspring cardiometabolic outcomes and postnatal growth trajectories after exposure to maternal SARS-CoV-2 infection. Preprint at medRxiv. <https://doi.org/10.1101/2023.08.16.23294170>.
118. Ockene, M.W., Russo, S.C., Lee, H., Monthé-Drèze, C., Stanley, T.L., Ma, I.L., Toribio, M., Shook, L.L., Grinspoon, S.K., Edlow, A.G., and Fourman, L.T. (2023). Accelerated Longitudinal Weight Gain Among Infants With In Utero COVID-19 Exposure. *J. Clin. Endocrinol. Metab.* 108, 2579–2588. <https://doi.org/10.1210/CLINEM/DGAD130>.
119. Abu-Raya, B., Michalski, C., Sadarangani, M., and Lavoie, P.M. (2020). Maternal Immunological Adaptation During Normal Pregnancy. *Front. Immunol.* 11, 575197. <https://doi.org/10.3389/fimmu.2020.575197>.
120. Erlebacher, A. (2013). Immunology of the maternal-fetal interface. *Annu. Rev. Immunol.* 31, 387–411. <https://doi.org/10.1146/annurev-immunol-032712-100003>.
121. Ritchie, M.E., Phipson, B., Wu, D., Hu, Y., Law, C.W., Shi, W., and Smyth, G.K. (2015). limma powers differential expression analyses for RNA-seq and microarray studies. *Nucleic Acids Res.* 43, e47. <https://doi.org/10.1093/NAR/GKV007>.
122. Orenbuch, R., Filip, I., Comito, D., Shaman, J., Pe'er, I., and Rabadan, R. (2020). arcasHLA: high-resolution HLA typing from RNAseq. *Bioinformatics* 36, 33–40. <https://doi.org/10.1093/BIOINFORMATICS/BTZ474>.
123. Gupta, N.T., Vander Heiden, J.A., Uduman, M., Gadala-Maria, D., Yaari, G., and Kleinstein, S.H. (2015). Change-O: a toolkit for analyzing large-scale B cell immunoglobulin repertoire sequencing data. *Bioinformatics* 31, 3356–3358. <https://doi.org/10.1093/BIOINFORMATICS/BTV359>.
124. Fajnzylber, J., Regan, J., Coxen, K., Corry, H., Wong, C., Rosenthal, A., Worrall, D., Giguel, F., Piechocka-Trocha, A., Atyeo, C., et al. (2020). SARS-CoV-2 viral load is associated with increased disease severity

- and mortality. *Nat. Commun.* **11**, 5493. <https://doi.org/10.1038/s41467-020-19057-5>.
125. Shook, L.L., Shui, J.E., Boatman, A.A., Devane, S., Croul, N., Yonker, L.M., Matute, J.D., Lima, R.S., Schwinn, M., Cvrk, D., et al. (2020). Rapid establishment of a COVID-19 perinatal biorepository: Early lessons from the first 100 women enrolled. *BMC Med. Res. Methodol.* **20**, 215. <https://doi.org/10.1186/s12874-020-01102-y>.
 126. BØYUM, A. (1976). Isolation of Lymphocytes, Granulocytes and Macrophages. *Scand. J. Immunol.* **5**, 9–15. <https://doi.org/10.1111/J.1365-3083.1976.TB03851.X>.
 127. Edlow, A.G., Li, J.Z., Collier, A.R.Y., Atyeo, C., James, K.E., Boatman, A.A., Gray, K.J., Bordt, E.A., Shook, L.L., Yonker, L.M., et al. (2020). Assessment of Maternal and Neonatal SARS-CoV-2 Viral Load, Transplacental Antibody Transfer, and Placental Pathology in Pregnancies During the COVID-19 Pandemic. *JAMA Netw. Open* **3**, e2030455. <https://doi.org/10.1001/JAMANETWORKOPEN.2020.30455>.
 128. Zheng, G.X.Y., Terry, J.M., Belgrader, P., Ryvkin, P., Bent, Z.W., Wilson, R., Ziraldo, S.B., Wheeler, T.D., McDermott, G.P., Zhu, J., et al. (2017). Massively parallel digital transcriptional profiling of single cells. *Nat. Commun.* **8**, 14049. <https://doi.org/10.1038/ncomms14049>.
 129. Li, B., Gould, J., Yang, Y., Sarkizova, S., Tabaka, M., Ashenberg, O., Rosen, Y., Slyper, M., Kowalczyk, M.S., Villani, A.C., et al. (2020). Cumulus provides cloud-based data analysis for large-scale single-cell and single-nucleus RNA-seq. *Methods* **17**, 793–798. <https://doi.org/10.1038/s41592-020-0905-x>.
 130. Heaton, H., Talman, A.M., Knights, A., Imaz, M., Gaffney, D.J., Durbin, R., Hemberg, M., and Lawnczak, M.K.N. (2020). Souporecell: robust clustering of single-cell RNA-seq data by genotype without reference genotypes. *Nat. Methods* **17**, 615–620. <https://doi.org/10.1038/s41592-020-0820-1>.
 131. Butler, A., Hoffman, P., Smibert, P., Papalexi, E., and Satija, R. (2018). Integrating single-cell transcriptomic data across different conditions, technologies, and species. *Nat. Biotechnol.* **36**, 411–420. <https://doi.org/10.1038/nbt.4096>.
 132. Korsunsky, I., Millard, N., Fan, J., Slowikowski, K., Zhang, F., Wei, K., Baglaenko, Y., Brenner, M., Loh, P.R., and Raychaudhuri, S. (2019). Fast, sensitive and accurate integration of single-cell data with Harmony. *Nat. Methods* **16**, 1289–1296. <https://doi.org/10.1038/s41592-019-0619-0>.
 133. Slowikowski, K. (2023). cellguide: Navigate single-cell RNA-seq datasets in your web browser. <https://doi.org/10.5281/ZENODO.8144195>.
 134. Liberzon, A., Birger, C., Thorvaldsdóttir, H., Ghandi, M., Mesirov, J.P., and Tamayo, P. (2015). The Molecular Signatures Database Hallmark Gene Set Collection. *Cell Syst.* **1**, 417–425. <https://doi.org/10.1016/J.CELS.2015.12.004>.
 135. Parlato, S., Chiacchio, T., Salerno, D., Petrone, L., Castiello, L., Romagnoli, G., Canini, I., Goletti, D., and Gabriele, L. (2018). Impaired IFN- α -mediated signal in dendritic cells differentiates active from latent tuberculosis. *PLoS One* **13**, e0189477. <https://doi.org/10.1371/JOURNAL.PONE.0189477>.
 136. Iwasaki, T., Watanabe, R., Ito, H., Fujii, T., Okuma, K., Oku, T., Hirayama, Y., Ohmura, K., Murata, K., Murakami, K., et al. (2022). Dynamics of Type I and Type II Interferon Signature Determines Responsiveness to Anti-TNF Therapy in Rheumatoid Arthritis. *Front. Immunol.* **13**, 901437. <https://doi.org/10.3389/FIMMU.2022.901437>.
 137. Yoshida, M., Worlock, K.B., Huang, N., Lindeboom, R.G.H., Butler, C.R., Kumasaka, N., Dominguez Conde, C., Mamanova, L., Bolt, L., Richardson, L., et al. (2021). Local and systemic responses to SARS-CoV-2 infection in children and adults. *Nature* **602**, 321–327. <https://doi.org/10.1038/s41586-021-04345-x>.
 138. McIver, L.J., Abu-Ali, G., Franzosa, E.A., Schwager, R., Morgan, X.C., Waldron, L., Segata, N., and Huttenhower, C. (2018). bioBakery: a meta'omic analysis environment. *Bioinformatics* **34**, 1235–1237. <https://doi.org/10.1093/BIOINFORMATICS/BTX754>.

STAR★METHODS

KEY RESOURCES TABLE

REAGENT or RESOURCE	SOURCE	IDENTIFIER
Antibodies		
Anti-Human CD3 AF700	Thermo Fisher Scientific	Cat# 56-0038-82; RRID: AB_906220
Anti-Human CD4 PE-Cy5 (Clone RPA-T4)	BioLegend	Cat# 300510; RRID: AB_314078
Anti-Human CD8 PE-Cy5.5 (Clone RPA-T8)	Thermo Fisher Scientific	Cat# 35-0088-42; RRID: AB_11218701
Anti-human CD19 BUV496 (Clone SJ25C1)	BD	Cat# 612938; RRID: AB_2870221
Anti-human HLA-DR FITC (Clone Tü36)	BioLegend	Cat# 361604; RRID: AB_2563165
Anti-human PD-1 BUV615 (Clone EH12.1)	BD	Cat# 612991; RRID: AB_2870262
Anti-human FOXP3 PE (Clone 206D)	BioLegend	Cat# 320108; RRID: AB_492986
Anti-human TIM-3 BUV737 (Clone 7D3)	BD	Cat# 748820; RRID: AB_2873223
Anti-human CD25 BV650 (Clone BC96)	BioLegend	Cat# 302634; RRID: AB_2563807
Anti-human TCR- $\gamma\delta$ BUV563 (Clone 11F2)	BD	Cat# 748534; RRID: AB_2872945
Anti-human IFN- γ BV750 (CloneB27)	BD	Cat# 566357; RRID: AB_2739707
Anti-human TNF- α FITC (CloneMab11)	BioLegend	Cat# 502906; RRID: AB_315258
Anti-human IL-2 BV605 (Clone JES6-5H4)	BioLegend	Cat# 503829; RRID:AB_11204084
Anti-human IL-4 BV786 (CloneMP4-25D2)	BD	Cat# 564113; RRID:AB_2738601
Anti-human Granzyme B BV421 (Clone QA18A28)	BioLegend	Cat# 396413; RRID: AB_2810602
Anti-human IL-17A PE-Cy7 (Clone eBio64DEC17)	Thermo Fisher Scientific	Cat# 25-7179-42; RRID: AB_11063994
Anti-human CD56 BV421 (Clone NCAM16.2)	BD	Cat# 562751; RRID: AB_2732054
Anti-human CD123 BUV805 (Clone 9F5)	BD	Cat# 742031; RRID: AB_2871327
Anti-human CD14 PE-Cy7 (Clone M5E2)	BioLegend	Cat# 301814; RRID: AB_389353
Anti-human CD16 BV785 (Clone3G8)	BioLegend	Cat# 302046; RRID: AB_2563803
Anti-human CD16 BUV805 (Clone3G8)	BD	Cat# 748850; RRID: AB_2873253
Anti-human CD45RO BUV661 (Clone UCHL1)	BD	Cat# 749887; RRID: AB_2874127
Anti-human CCR7 CF-594 (Clone 2-L1-A)	BD	Cat# 566768; RRID: AB_2869857
Anti-human CD38 BV750 (Clone HIT2)	BD	Cat# 746909; RRID: AB_2871703
Anti-human CD66b PerCP-Cy5.5 (Clone G10F5)	BioLegend	Cat# 305108; RRID: AB_2077855
Human BD Fc Block™ (Clone Fc1)	BD	Cat# 564219; RRID: AB_2728082
TotalSeq antibodies for CITE-seq	BioLegend	See Table S11
Biological samples		
PBMCs from healthy non-pregnant, non-pregnant COVID-19, non-pregnant convalescent, healthy pregnant, pregnant COVID-19 and pregnant convalescent	This study	N/A
Plasma from healthy non-pregnant, non-pregnant COVID-19, healthy pregnant, pregnant COVID-19	This study	N/A
Stool specimen from, non-pregnant COVID-19, healthy pregnant, pregnant COVID-19	This study	N/A
Chemicals, peptides, and recombinant proteins		
eBioscience™ Cell Stimulation Cocktail (plus protein transport inhibitors)	Thermo Fisher Scientific	00-4975-03
FBS	Hyclone	Cat# SH30910.03
2- mercaptoethanol	Thermo Fisher Scientific	21985023
LPS	Milipore-Sigma	L2630-10MG
Glycophorin A-based antibody kit	Stemcell Technologies	01738

(Continued on next page)

Continued

REAGENT or RESOURCE	SOURCE	IDENTIFIER
TruStain FcX blocker	BioLegend	422302
MojoSort CD45 Nanobeads	BioLegend	480030
Hashtag antibodies	BioLegend	Table S11
Annexin-V-conjugated bead kit	Stemcell Technologies	17899
Heat-inactivated human AB serum	Milipore-Sigma	H3667-20ML
Critical commercial assays		
Human Cytokine/Chemokine 71-Plex Discovery Assay (HD71)	Eve Technologies	HD71
LEGENDplex™ Human Cytokine Panel 2 (13-plex)	BioLegend	Cat# 740102
LEGENDplex™ Human Anti-Virus Response Panel (13-plex)	BioLegend	Cat# 740390
LEGENDplex™ Human Cytokine Panel 2 (13-plex)	BioLegend	Cat# 740985
CD14 MicroBeads, human	Miltenyi Biotec	–
Chromium Single Cell 5' kit	V2 NextGEM 10X Genomics	PN-1000263
5' Feature Barcode library kit	10X Genomics	PN-1000256
Chromium Single Cell V(D)J Enrichment kit	10 Genomics	PN-1000252, PN-1000253
AllPrep PowerFecal DNA/RNA 96 Kit	Qiagen	80254
Nextera XT DNA library preparation kit	Illumina	FC-131-1024
LIVE/DEAD Fixable Aqua Dead Cell stain kit	Thermo Fisher Scientific	Cat# L34966
FoxP3 transcription factor staining kit	Thermo Fisher Scientific	Cat# 00-5523-00
Deposited data		
scRNA data, CITE-seq, and repertoire data	This study	GEO: GSE239452
Code used for single-cell analysis and figures generation	This study	https://github.com/villani-lab/COVID_pregnancy
Software and algorithms		
Flowjo 10	BD	https://www.flowjo.com
Prism 9	Graphpad	https://www.graphpad.com
Cell Ranger v6.0.1	10x Genomics	https://support.10xgenomics.com/single-cell-gene-expression/software/pipelines/latest/what-is-cell-ranger
Terra platform	–	https://app.terra.bio/
Souporcell ¹²¹ v2.0 (python)	Heaton, H et al. ¹²¹	https://github.com/wheaton5/souporcell
Pegasus v1.7.1 (python)	–	https://github.com/lllab-bcb/pegasus/tree/master
scanpy V1.9.3 (python)	F. Alexander Wolf et al. ¹²¹	https://github.com/scverse/scanpy
Full python package list with versions	See Table S12	–
Limma package v3.54.2 (R)	Ritchie, M.E et al. ¹²²	https://bioconductor.org/packages/release/bioc/html/limma.html
ArcasHLA v0.5.0 (R)	Orenbuch, R et al. ¹²²	https://github.com/RabadanLab/arcasHLA
Alakazam v1.2.1 (R)	Gupta, N.T et al. ¹²³	https://github.com/cran/alakazam
bioBakery 3 shotgun metagenome workflow 3.0.0	–	https://github.com/biobakery/biobakery_workflows
KneadData 0.10.0	–	https://pypi.org/project/kneaddata/
MetaPhlan 3.0.0	–	https://huttenhower.sph.harvard.edu/metaphlan3/

EXPERIMENTAL MODEL AND STUDY PARTICIPANT DETAILS

Human participants and data collection

Pregnant women receiving care at Massachusetts General Hospital and Brigham and Women's Hospital in Boston, MA, and enrolled in a COVID-19 pregnancy biorepository between April 2020 and January 2021, prior to the widespread availability of COVID-19

vaccines, were included in this study (MGB IRB#2020P003538 and #2020P000804). Pregnant women were eligible for inclusion if they were 18 years of age or older, able to provide informed consent for themselves or with a healthcare proxy, and diagnosed with, or at risk for SARS-CoV-2 virus infection. All participants were tested for the presence of SARS-CoV-2 by RT-PCR of nasopharyngeal swabs on admission to Labor and Delivery per hospital infection control policy. Patients were also tested if they had symptoms of COVID-19, even if they had not been admitted to Labor and Delivery. Contemporaneous uninfected pregnant individuals (again status confirmed by SARS-CoV-2 RT-PCR of nasopharyngeal swab) were also enrolled at delivery. Individuals with autoimmune disease/use of immune-modulating medications, and those with other infections, such as clinical chorioamnionitis, or other symptoms of viral or bacterial infection were also excluded.

Non-pregnant women hospitalized with confirmed SARS-CoV-2 infection and enrolled contemporaneously as part of a general adult cohort described previously¹²⁴ (MGB IRB #2020P000804) were used as an additional comparator group. Banked PBMC and plasma samples from healthy, non-pregnant, control women collected prior to the COVID-19 pandemic were used as an additional biological comparator group. These participants were known to be negative for HIV, TB, EBV, Hepatitis B and C, and Dengue virus, with normal complete blood counts and not on any immune-modulating medications; their samples were collected as part of a protocol (MGB IRB # 2010P002121) to bank healthy control samples for use as biological comparators in infectious disease studies.

Clinical and sample definitions

Clinical and demographic information were abstracted from the electronic medical record. COVID-19 symptom severity was determined based on NIH criteria.^{47,48} Samples not designated “convalescent” were collected from pregnant participants in closest proximity to acute COVID-19 illness and within 30 days of a positive SARS-CoV-2 test. Samples from uninfected pregnant participants, and from convalescent individuals who tested positive for SARS-CoV-2 infection during pregnancy but remote (>30 days) from delivery sample collection, were collected during the delivery hospitalization on admission to Labor and Delivery. Details on sample collection procedures have been described previously.¹²⁵

METHOD DETAILS

Blood specimen processing

Blood samples were obtained by venipuncture into EDTA tubes. Blood was centrifuged at $1000 \times g$ for 10 min, and plasma was aliquoted and stored at -80°C . PBMCs were collected using a Ficoll density gradient.¹²⁶ Briefly, blood was transferred to a 50 mL conical tube and diluted 1:1 with Hanks' balanced salt solution (HBSS) without calcium or magnesium. Diluted blood was layered on top of Ficoll in a 2:1 ratio. The conical tube was then centrifuged at $1000 \times g$ for 30 min at room temperature without braking. The interphase was collected and placed in a new 15 mL conical tube with HBSS to bring the volume to 15 mL and centrifuged at $330 \times g$ for 10 min with high brake. The supernatant was removed and the cell pellet washed with HBSS. Cells were frozen in freezing medium with RPMI 1640 medium with 1% penicillin-streptomycin, L-glutamine, 1% sodium pyruvate, 1% non-essential amino acids, 20% FBS, and 10% DMSO at 5–10 million cells/cryovial, placed in a chilled Mr. Frosty, stored at -80°C for one day, then transferred to liquid nitrogen for long-term storage.

Flow cytometry-based immune cell profiling

PBMCs were plated at 1×10^6 cells per well in a 96-well U-bottom plate. PBMCs were stimulated with eBioscience Cell Stimulation Cocktail (plus protein transport inhibitors) (Thermo Fisher Scientific) in RPMI (RPMI-1640 supplemented with 10% fetal bovine serum (FBS), 2 mM L-glutamine, 100 U/ml penicillin, and 100 mg/mL streptomycin, 1 mM sodium pyruvate, and 50 μM 2-mercaptoethanol) for 5 h to monitor cytokine expression. After stimulation, cells were stained with antibodies against cell-surface markers and the LIVE/DEAD fixable dye Aqua (Thermo Fisher Scientific) to exclude dead cells, fixed and permeabilized with a FoxP3 transcription factor staining kit (Thermo Fisher Scientific), and subsequently stained with cytokine- and/or transcription factor-specific antibodies. All flow cytometry analyses were performed on a Symphony flow cytometer (BD), and data were analyzed with FlowJo software (BD). The specific markers used to identify each subset of cells are summarized in the gating strategy (Figure S1). Antibodies that were used for flow cytometry are listed in the STAR Methods Antibodies Table.

Monocyte enrichment and stimulation

PBMC numbers were counted, and 2×10^6 of PBMCs were used to enrich for CD14⁺ monocytes with MACS microbeads system (Miltenyi Biotec) according to the manufacturer's protocol. 1×10^5 cells of MACS-sorted CD14⁺ monocytes were stimulated with 1 ng/mL LPS in 200 μL of 10%FBS RPMI-1640 media for 8 h. After stimulation, cells were centrifuged, and supernatants were kept at -80°C for the downstream analysis.

Cytometric bead array

Cytokine and chemokine concentrations were measured from the supernatants of CD14⁺ monocytes by cytometric bead array according to the manufacturer's protocol (BioLegend).

Plasma cytokine and chemokine analysis

Plasma samples were collected from 38 pregnant patients with acute COVID-19, 31 non-pregnant with acute COVID-19, 21 SARS-CoV-2 negative uninfected pregnant controls, and 17 uninfected non-pregnant controls. Plasma samples were shipped to Eve Technologies (Calgary, Alberta, Canada) on dry ice, and levels of cytokine, chemokine, and growth factor were measured with Human Cytokine/Chemokine 71-Plex Discovery Assay (HD71). Serum levels of IL-1RA were validated by an IL-1RA Human ELISA Kit (Invitrogen).

Single-cell cohort details

Samples from pregnant participants collected as part of a healthcare-system-wide COVID pregnancy biorepository described previously^{125,127} were selected for single-cell sequencing to span a range of disease severity as follows: 3 samples from healthy uninfected pregnant “control” participants at term (39–40 weeks), 3 samples from asymptomatic pregnant SARS-CoV-2 positive individuals who tested positive at universal screening upon hospital admission (34, 39 and 40 weeks), and 3 samples from pregnant individuals PCR positive for SARS-CoV-2 with severe or critical COVID-19 as defined by NIH criteria⁴⁸ (2 critically-ill at 34 and 41 week, 1 severe at 36 weeks). All included samples were collected prior to the initiation of any treatment.

The non-pregnant participants were selected from an MGH COVID-19 patient cohort described previously.⁶⁴ Out of this large cohort we chose the “non-pregnant severe” sample group by the following criteria: samples of female patients, 20–34 years old, PCR positive for SARS-CoV-2 with severe or critical COVID-19 by NIH criteria,⁴⁸ The “non-pregnant asymptomatic” sample group was selected by the following criteria: samples of female patients, 20–34 years old, PCR positive for SARS-CoV-2, without symptoms (none of these patients were admitted to the hospital within a 28 day window, all survived). All included samples were from day 0 before any treatment started. Further meta-data is available in [Table S3](#).

PBMC CD45⁺ enrichment, cell hashing, CITE-seq staining

Cryopreserved PBMC samples (total of nine samples from the MGH pregnancy cohort and 17 samples from the MGH COVID-19 acute cohort) were thawed at 37°C, diluted with a 10x volume of RPMI with 10% heat-inactivated human AB serum (Sigma Aldrich), and centrifuged at 300 × *g* for 7 min. Cells were resuspended in CITE-seq buffer (RPMI with 2.5% [v/v] human AB serum and 2 mM EDTA) and added to 96-well plates. Dead cells were removed with an Annexin-V-conjugated bead kit (Stemcell Technologies, 17899) and red blood cells were removed with a glycophorin A-based antibody kit (Stemcell Technologies, 01738); modifications were made to the manufacturer’s protocols for each to accommodate a sample volume of 150 μL. Cells were quantified with an automated cell counter (Bio-Rad, TC20), after which, 2.5 × 10⁵ cells were resuspended in CITE-seq buffer containing TruStain FcX blocker (BioLegend, 422302) and MojoSort CD45 Nanobeads (BioLegend, 480030). Hashtag antibodies (BioLegend) were added to samples ([Table S11](#)) followed by a 30 min incubation on ice. Cells were then washed three times with CITE-seq buffer using a magnet to retain CD45⁺ cells. Live cells were counted with trypan blue, and samples from each cohort bearing different hashtag antibodies were pooled together at equal concentrations.

For the pregnancy cohort, three pools of three samples across COVID-19 severity (severe COVID-19, asymptomatic SARS-CoV-2 infection, and no-SARS-CoV2 infection) were pooled (three pools) and loaded on three channels (total of nine channels), and the data from each donor and each channel was concatenated for computational analysis. For the MGH acute cohort, samples were pooled in groups of eight and loaded on two channels; individual donors selected as controls from the acute cohort were age- and gender-matched to the participants in the pregnancy cohort. Pooled samples were filtered with 40 μM strainers, centrifuged, and resuspended in CITE-seq buffer with TotalSeq-C antibody cocktail (BioLegend; [Table S11](#)). Cells were incubated on ice for 30 min, followed by three washes with CITE-seq buffer and a final wash in the same buffer without EDTA (RPMI with 2.5% [v/v] human AB serum). Cells were resuspended in this buffer without EDTA, filtered a second time, and counted.

Single-cell gene expression, feature bar code, and TCR/BCR library construction and sequencing

An input of 50,000 hashed PBMC samples was loaded on a single channel in the 10X Chromium instrument for blood immune cell analysis, aiming for a recovery goal of 25,000 single cells. Hashed PBMC single-cell libraries were generated with the Chromium Single Cell 5’ kit (V2 NextGEM 10X Genomics, PN-1000263) together with the 5’ Feature Barcode library kit (10X Genomics PN-1000256). PCR-amplified cDNA was used for TCR and BCR enrichment with the Chromium Single Cell V(D)J Enrichment kit (10 Genomics PN-1000252 and PN-1000253). The library quality was assessed with an Agilent 2100 Bioanalyzer. All gene expression, feature barcode, TCR and BCR libraries were sequenced on an Illumina NovaSeq using the S4 300 cycles flow with the following sequencing parameters: read 1 = 26; read 2 = 90; index 1 = 10; index 2 = 10. Measurements from the three modalities were measured in the same cells and could be associated using the cell barcode.

scRNA-seq read alignment and quantification

RNA data

Raw sequencing data was pre-processed with CellRanger (v6.0.1, 10x Genomics) to demultiplex FASTQ reads, align reads to the human reference genome (GRCh38), and count unique molecular identifiers (UMI) to produce a cell × gene count matrix.¹²⁸ We used the Terra platform (<https://app.terra.bio/>) to run Cell Ranger via the workflow script that is part of a collection called Cumulus.¹²⁹ All samples were genetically demultiplexed using SoupCell¹³⁰ (v2.0). Hashtag oligos (HTOs) were demultiplexed by Pegasus

(v1.7.1, python) functions estimate_background_probs and demultiplex. Soupورcells' assignments were mapped to the demultiplexed HTOs of patients to identify the Soupورcell assignment of the genetically demultiplexed samples. We used the results from the genetic demultiplexing because they resulted in fewer “doublet” and “unknown” assignments.

All count matrices were then aggregated with Pegasus using the aggregate_matrices function. Low-quality droplets were filtered out of the matrix prior to proceeding with downstream analyses using the percent of mitochondrial UMIs and number of unique genes detected as filters (<20% mitochondrial content, >300 unique genes). The percent of mitochondrial UMI was computed using 13 mitochondrial genes (MT-ND6, MT-CO2, MT-CYB, MT-ND2, MT-ND5, MT-CO1, MT-ND3, MT-ND4, MT-ND1, MT-ATP6, MT-CO3, MT-ND4L, MT-ATP8) using the qc_metrics function in Pegasus. The counts for each remaining cell in the matrix were then log-normalized by computing the log_{1p} (counts per 100,000), which we refer to in the text and figures as log(CPM).

Protein data

Antibody-derived tags (ADT) data was demultiplexed by matching cell barcodes of the protein data to that of the RNA data cell barcodes. Only cells that had RNA data were paired with the protein data, we did not include cells that had only protein data without a matching RNA data. Protein data demultiplexing was therefore projected from the RNA-based demultiplexing. All protein values were CLR¹³¹ (centered log ratio) transformed by the following formula where x denotes an ADT vector of a single cell c and G_c is the gene expression of all genes for cell c :

$$s(x_c) = \sum_{g \in G_c} \log(g|g > 0)$$

$$CLR(x_c) = \log(x / e^{s(x)/len(x)})$$

Basic and lineage-level single-cell clustering

All cells from all samples after the above-mentioned filtering were used for clustering. We identified candidates for highly variable genes as those that are expressed in at least 5% of the cells. Then, 2,000 highly variable genes (HVGs) were selected using the highly_variable_features function in Pegasus and used as input for principal component analysis. TCR and BCR genes were pre-excluded from the candidate HVGs. To account for batch effects, the resulting principal component scores were aligned using the Harmony algorithm.¹³² The resulting principal components were used as input for Leiden clustering and Uniform Manifold Approximation and Projection (UMAP) algorithm. We identified main lineages using marker genes: T/NK cells (CD3E, CD3D, CD8A, CD8B, CD4, NCAM1, FCGR3A), B and plasma cells (MS4A1, CD19, JCHAIN) and MNP (VCAN, LYZ, CD136, MARCO, CD14, HLA-DRB1, HLA-DRA). To further split CD4 T cells from CD8 T cells, we had to further split the T/NK subset by CD4, CD8, CD3E, CD3D, and NCAM1 (Figures S6H and S6I). In the resulting embedding and clustering (Figure S6H) clusters 4, 5, 7, 13, 16, and 17 were accounted as CD4 T cells and were re-sub-clustered (Figure 4E); clusters 1, 2, 3, 9, 10, 11, 12, 14, 15, 18 were accounted as CD8⁺ T cells (Figure S6H) and were re-sub-clustered (Figure 3A); and clusters 6 and 8 were accounted as NK cells (Figure S6H). Of note, some NK cells were found in the CD8 T cell lineage and were annotated as such. For every lineage separately we re-ran the clustering procedure: identified 1,000 HVGs, ran PCA, computed a UMAP embedding based on 50 PCs, and clustered using the Leiden algorithm.

Single-cell subset annotation

To annotate cell subsets at the lineage-level clustering, we used two complementary methods to identify marker genes and proteins: “one versus all” (OVA) in which we test which genes are differentially expressed between each cluster and the rest of the cells that do not belong to it; and “all versus all” (AVA) in which we test which genes are differentially expressed between every pair of clusters. For OVA, we calculated the area under the receiver operating characteristic (AUROC) curve for the log(CPM) values of each gene as a predictor of cluster membership using the de_analysis function in Pegasus. Genes with an AUROC ≥ 0.75 were considered as marker genes for a particular cell subset. In addition, we computed a pseudo-bulk count matrix by counting UMIs for every patient in every cluster. We then tested for differential gene expression between clusters using the Limma package (v3.54.2, R)¹²¹ and modeling gene \sim is_clust using the lmFit() function, where is_clust is a factor with levels indicating if the sample was or was not in the subset being tested. For AVA, we used the pseudo-bulk matrix to model the gene expression in each cluster separately gene \sim clust using the lmFit() function, where clust denotes the cluster, we then contrasted every cluster with every other cluster in this model using Limma's contrasts.fit() function. The pseudo-bulk and AUROC statistics of OVA differentially expressed genes (DEGs) for all cell subsets can be found in Table S10.

Marker genes for each cell subset were interrogated and investigated for several different cluster resolutions using Cell Guide.¹³³ For each lineage, we identified the final resolution in which every cluster has a unique set of marker genes differentiating it from the rest of the clusters. Table S4 details the main gene and protein markers that were used to annotate every cell subset. If two cell clusters were indistinguishable, they were merged to create one cell subset to obtain the best possible resolution. The numbering of cell subsets in every lineage was finalized to be sorted by the cell subset size. The resolutions used for the final lineage clustering were as follows: T/NK cells resolution = 1.8, CD4 T cells resolution = 1, MNPs resolution = 1, B/Plasma cells resolution = 1.3. We annotated doublets and low-quality cell subsets as such in every lineage they were identified. Low quality cell subsets include subsets with high-mitochondrial content or high ribosomal content that might be indicative of dying cells. We did not remove them from the

anndata objects or the UMAP embeddings to allow different interpretations by others who may use this data in the future. We *did* exclude low-quality cell subsets from all downstream analysis in this manuscript such as differential abundance, differential gene expression or enrichment of expanded clones.

Single-cell differential abundance analysis

To test differential abundances in different cell subsets across conditions, we computed the abundance of each cell subset in every patient and tested differential abundance by Mann-Whitney U test across desired conditions. We then corrected for multiple hypotheses using Benjamini-Hochberg FDR for every lineage separately. We compared the different conditions we have in our single-cell cohort in two main levels: the first is comparing the finest resolution we have - pregnant-control/pregnant-asymptomatic/pregnant-severe/non-pregnant-asymptomatic/non-pregnant-severe. Since the sample size of these groups is limited, the majority of the comparisons came up as insignificant (Figures S6E, S6K, S7C, S8B, S9D, and S10G). We, therefore, then tested differential abundance at a lower resolution by grouping all pregnant COVID-19 patient samples (pregnant-asymptomatic and pregnant-severe) and compared them to all non-pregnant COVID-19 patient samples (non-pregnant-asymptomatic and non-pregnant-severe) in which some cell subsets showed differential abundance (Figures 3B, 4I, S7B, S8C and S10F). We excluded doublets and low-quality cell subsets for the differential abundance analysis.

Repertoire analysis

Clone definitions, frequency of clones

A clone was defined by concatenating the following sequences that are the output of CellRanger for T cells: TRA_cdr3, TRB_cdr3, TRA_v_gene, TRB_v_gene, TRA_j_gene, TRB_j_gene; and for B cells: IGL_cdr3, IGK_cdr3, IGH_cdr3, IGL_v_gene, IGK_v_gene, IGH_v_gene, IGL_j_gene, IGK_j_gene, IGH_j_gene. Any cell that lacked any one of the above components was defined as having no clone information.

Clone frequency is defined as the ratio between the number of single cells with the exact same clone sequence for a patient and the total number of cells with TCR/BCR information for that patient (cells that have TCR/BCR information are illustrated in, Figures S7D, S8D, and S10A).

An expanded clone is defined as a clone with a frequency of at least 1% out of a sample and that appears in at least 5 single cells in that sample.

Enrichment of TCR/BCR clones in cell subsets

To identify enrichment of expanded clones in cell subsets in different conditions, we defined the frequency of expanded clones per cell subset per patient by

$$freq_{S,c} = \frac{n_{c,S}}{N_S}$$

Where $n_{c,S}$ is the total number of cells that are part of an expanded clone in sample S in cluster c

N_S is the total number of cells that are part of an expanded clone in sample S

We then compared $freq_{S,c}$ across different conditions and used Mann-Whitney U test and Benjamini-Hochberg multiple hypothesis correction to test if they differ significantly (Figures 3D, S10F, and S10G;). We excluded doublets and low-quality cell subsets from this analysis.

Putative epitopes for CD8 TCRs

We downloaded the VDJdb⁸³ database in February 2023 and queried it to identify putative epitopes for the CD8 TCRs identified in our data using an R script.

HLA alleles

In an attempt to make the putative epitopes found by VDJdb more specific (in the first query of VDJdb several epitopes were found for most TCRs), we sought to identify HLA alleles per patient and rerun the VDJdb query. To identify HLA alleles, we used the functions `extract()` and `genotype()` from the repo ArcashHLA¹²² (v0.5.0, R).

TCR sequence diversity

Diversity curves that measured Hill's diversity metric across diversity orders 0–4 were created using the package `alakazam`¹²³ (v1.2.1, R) with the `alphaDiversity` function. Hill's diversity metric was only calculated on samples with ≥ 200 total TCR sequences. We tested the differences between the diversity index in $q = [0,1,2,3,4]$ by a Mann-Whitney test.

ISG expression analysis

We compiled an initial ISG list by incorporating the Molecular Signature Database (MSigDB)¹³⁴ Interferon Alpha Response gene set, MSigDB Interferon Gamma Response gene set, and gene sets that were previously shown to take part in inflammatory and auto-immune responses in humans.^{135–137} This initial list consists of 270 genes. We tested for differential gene expression between pregnant

patients with COVID-19 and non-pregnant patients with COVID-19 by testing the difference in expression per gene per cell subset using Mann-Witney test and Benjamini-Hochberg multiple hypothesis testing across all ISGs for every cell subset (Table S5). We then identified significant gene-(cell subset) pairs as those with an absolute $\log_{10}(\text{fold-change}) > 0.2$ (absolute $\log_{10}(\text{fold-change}) > \sim 1.58$) and adjusted $p\text{-value} < 0.05$. We filtered out genes that had no cell subset in which they are differentially expressed between pregnant and non-pregnant patients with COVID-19. We were left with 91 ISGs that showed significant differences in at least 1 cell subset. $\log_{10}(\text{fold-change})$ of this differential expression analysis was truncated at 1 and -1: any values greater than 1 were converted to 1 and any values lower than (-1) were converted to (-1) (Figure S10). We excluded doublets and low-quality cell subsets from this analysis.

Metagenomic analysis

Fresh stool samples were collected and refrigerated at 4°C until aliquoting and freezing at -80°C, typically within 4 h of collection. Nucleic acids were extracted from stool samples using the AllPrep PowerFecal DNA/RNA 96 Kit (Qiagen) and metagenomes were sequenced at the Broad Institute, according to their standard established platforms. Briefly, DNA was prepared for sequencing using the Illumina Nextera XT DNA library preparation kit and sequenced with a target of 3GB output at 2 × 150 bp read length using the NovaSeq platform (Illumina). Taxonomic profiles were generated using the bioBakery 3 shotgun metagenome workflow 3.0.0, which has previously been described.¹³⁸ Human reads were filtered using KneadData 0.10.0 and taxonomic profiles were generated using MetaPhlan 3.0.0.

QUANTIFICATION AND STATISTICAL ANALYSIS

Statistical analyses were performed with PRISM 9. Each data point denotes individual human subjects or animals. For Figures 1, 2, 3, S2–S5, S11, S14 and S15 statistical significance was calculated by Mann-Whitney non-parametric test for comparisons between the non-pregnant and pregnant groups in the same disease severity, and Kruskal-Wallis non-parametric test for comparisons within the non-pregnant or pregnant group. $p\text{-values}$ were shown after multiple hypotheses correction by Dunn's. For the boxplots in Figures 3, 4, and S6–S10, each dot represents a patient, the box limits represent the 25th and 75th percentiles of the data distribution (inter-quartile range, IQR), the line in the middle of the box represents the median and the whiskers represent data points up to 1.5*IQR. Dots beyond the whiskers are considered outliers and are marked by a diamond. Statistical testing - Mann-Whitney U test; $p\text{-values}$ were shown after multiple hypotheses correction by Benjamini-Hochberg; (ns) denotes not significant after multiple hypotheses correction.